Uncovering the Computational Mechanisms Underlying Many-Alternative Choice

Armin W. Thomas [1,2,3,4], Felix Molter [3,4,5], Ian Krajbich [6*]

1 Max Planck Institute for Human Development, Berlin, Germany

2 Technische Universität Berlin, Berlin, Germany

3 Freie Universität Berlin, Berlin, Germany

4 Center for Cognitive Neuroscience Berlin, Berlin, Germany

5 WZB Berlin Social Science Center, Berlin, Germany

6 The Ohio State University, Columbus, OH, USA

* Correspondence concerning this article should be addressed to Ian Krajbich (krajbich@gmail.com)

Armin W. Thomas, Center for Lifespan Psychology, Max Planck Institute for Human Development, Lentzeallee 94, 14195 Berlin, Germany; Felix Molter, School of Business & Economics, Freie Universität Berlin, Garystr. 21, 14195 Berlin, Germany; Ian Krajbich, Department of Psychology, Department of Economics, The Ohio State University, 1827 Neil Avenue, 200E Lazenby Hall, Columbus Ohio 43210, USA.

Abstract

How do we choose when confronted with many alternatives? There is surprisingly little decision modeling work with large choice sets, despite their prevalence in everyday life. Even further, there is an apparent disconnect between research in small choice sets, supporting a process of gaze-driven evidence accumulation, and research in larger choice sets, arguing for models of optimal choice, satisficing, and hybrids of the two. Here, we bridge this divide by developing and comparing different versions of these models in a many-alternative value-based choice experiment with 9, 16, 25, or 36 alternatives. We find that human choices are best explained by models incorporating an active effect of gaze on subjective value. A gaze-driven, probabilistic version of satisficing generally outperforms the other models, though gaze-driven evidence accumulation and comparison performs comparably well with 9 alternatives and is overall most accurate in capturing the relation between gaze allocation and choice.

Keywords. decision making, many-alternative forced choice, eye movements, gaze bias, evidence accumulation, satisficing

Introduction

In everyday life, we are constantly faced with value-based choice problems involving many possible alternatives. For instance, when choosing what movie to watch or what food to order off a menu, we must often search through a large number of alternatives. While much effort has been devoted to understanding the mechanisms underlying two-alternative forced choice (2AFC) in value-based decision-making (Alós-Ferrer, 2018; Bhatia, 2013; Boorman, Rushworth & Behrens, 2013; Clithero, 2018; De Martino, Kumaran, Seymour, & Dolan, 2006; Hare, Camerer & Rangel, 2009; Hunt, Malalasekera, de Berker, Miranda, Farmer, et al., 2018; Hutcherson, Bushong & Rangel, 2015; Krajbich, Armel & Rangel, 2010; Mormann, Malmaud, Huth, et al., 2010; Philiastides & Ratcliff, 2013; Polonia, Woodford & Ruff, 2019; Rodriquez, Turner & McClure, 2014; Webb. 2019) and choices involving three to four alternatives (Berkowitsch, Scheibehenne & Rieskamp, 2014; Diederich, 2003; Gluth, Spektor & Rieskamp, 2018; Gluth, Kern, Kortmann & Vitali, 2020; Krajbich & Rangel, 2011; Noguchi & Stewart, 2014; Roe, Busemeyer & Townsend, 2001; Towal, Mormann, & Koch, 2013; Trueblood, Brown & Heathcote, 2014; Usher & McClelland, 2004), comparably little has been done to investigate many-alternative forced choices (MAFC, more than four alternatives) (Ashby, Jekel, Dickert & Glöckner, 2016; Payne, 1976; Reutskaja, Nagel, Camerer, & Rangel, 2011).

Prior work on 2AFC has indicated that simple value-based choices are made through a process of gaze-driven evidence accumulation and comparison, as captured by the attentional drift diffusion model (aDDM; Krajbich, Armel & Rangel, 2010; Krajbich & Rangel, 2011; Smith & Krajbich, 2019) and the gaze-weighted linear accumulator model (GLAM; Thomas, Molter, Krajbich et al., 2019). These models assume that noisy evidence in favor of each alternative is compared and accumulated over time. Once enough evidence is accumulated for one alternative relative to the others, that alternative is chosen. Importantly, gaze guides the accumulation process, with temporarily higher accumulation rates for looked-at alternatives. One result of this process is that longer gaze towards one alternative should generally increase the probability that it is chosen, in line with recent empirical findings (Amasino, Sullivan, Kranton & Huettel, 2019; Armel, Beaumel & Rangel, 2008; Cavanagh, Wiecki, Kochar, & Frank, 2014; Fisher, 2017; Folke, Jacobsen, Fleming, & De Martino, 2017; Gluth et al., 2018, 2020; Konovalov & Krajbich, 2016; Pärnamets, Johansson, & Hall et al., 2015; Shimojo, Simion, Shimojo, & Scheier, 2003; Stewart, Hermens & Matthews, 2016; Vaidya & Fellows, 2015). While this framework can in theory be extended to MAFC (Gluth et al., 2020; Krajbich & Rangel, 2011; Thomas et al., 2019; Towal et al., 2013), it is still unknown whether it can account for choices from truly large choice sets.

In contrast, past research in MAFC suggests that people may resort to a "satisficing" strategy. Here, the idea is that people set a minimum threshold on what they are willing to accept and search through the alternatives until they find one that is above that threshold (McCall, 1970; Simon, 1955, 1956, 1957, 1959; Schwartz, Ward, Monterosso et al., 2002; Stüttgen, Boatwright & Monroe, 2012). Satisficing has been observed in a variety of choice scenarios, including tasks with a large number of alternatives (Caplin, Dean, & Martin, 2011; Stüttgen et al., 2012), patients with damage to the prefrontal cortex (Fellows, 2006), inferential decisions (Gigerenzer & Goldstein, 1996), survey questions (Krosnick, 1991), risky financial decisions (Fellner, Güth, & Maciejovsky, 2009), and with increasing task complexity (Payne, 1976). Past work has also investigated MAFC under strict time limits (Reutskaja et al., 2011). There, the authors find that the best model is a probabilistic version of satisficing in which the time point when individuals stop their search and make a choice follows a probabilistic function of elapsed time and cached (i.e., highest-seen) item value (Chow & Robbins, 1961; Rapoport & Tversky, 1966; Robbins, Sigmund & Chow, 1971; Simon, 1955, 1959).

There is some empirical evidence that points towards a gaze-driven evidence accumulation and comparison process for MAFC. For instance, individuals look back and forth between alternatives as if comparing them (Russo & Rosen, 1975). Also, frequently looking at an item dramatically increases the probability of choosing that item (Chandon, Hutchinson, Bradlow, & Young, 2009). Empirical evidence has further indicated that individuals use a gaze-dependent evidence accumulation process when making choices from sets of up to eight alternatives (Ashby et al., 2016).

Here, we sought to study the mechanisms underlying MAFC, by developing and comparing different decision models on choice, response-time (RT), liking rating, and gaze data from a choice task with sets of 9, 16, 25, and 36 snack foods. These models combine an either passive or active account of gaze in the decision process with three distinct accounts of the decision mechanism, namely probabilistic satisficing and two variants of evidence accumulation, which either perform relative comparisons between the alternatives or evaluate each alternative independently.

In terms of overall goodness-of-fit, we find that the models with active gaze consistently outperform their passive-gaze counterparts. That is, gaze does more than bring an alternative into the consideration set, it actively increases the subjective value of the attended alternative. The probabilistic satisficing model consistently performs best at capturing individuals' choices and RTs, with the relative accumulator model performing comparably well with 9 alternatives, but then falling behind for larger sets. Additionally, relative accumulation steadily loses ground to independent accumulation as the set sizes increase. Nevertheless, relative accumulation provides the overall best account of the empirically observed positive relation of gaze allocation and choice behaviour.

Results

Experiment design

Figure 1. Choice task. A: Subjects chose a snack-food item (e.g., chocolate bars, chips, gummy bears) from choice sets with 9, 16, 25, or 36 items. There were no time restrictions during the choice phase. Subjects indicated when they had made a choice by pressing the spacebar of a keyboard in front of them. Subsequently, subjects had 3 seconds to indicate their choice by clicking on their chosen item with a mouse cursor that appeared at the center of the screen. Subjects used the same hand to press the space bar and navigate the mouse cursor. For an overview of the choice indication times (defined as the time difference between the space bar press and the click on an item), see Figure 1-figure supplement 1. Trials from the four set sizes were randomly intermixed. Before the beginning of each choice trial, subjects had to fixate a central fixation cross for 0.5 s. Eye movement data were only collected during the central fixation and choice phase. B: After completing the choice task, subjects indicated how much they would like to eat each snack food item on a 7-point rating scale from -3 (not at all) to 3 (very much). For an overview of the liking rating distributions, see Figure 1-figure supplement 2-3. The tasks used real food items that were familiar to the subjects.

In each of 200 choice trials, subjects (N = 49) chose which snack food they would like to eat at the end of the experiment, out of a set of either 9, 16, 25, or 36 alternatives (50 trials per set size condition; see Fig. 1 and “Methods”). We recorded subjects’ choices, RTs, and eye-movements. After the choice task, subjects also rated each food on an integer scale from -3 (i.e., not at all) to +3 (i.e., very much) to indicate how much they would like to eat each item at the end of the experiment (for an overview of the liking rating distributions, see Figure 1-figure supplement 2-3).

Visual search

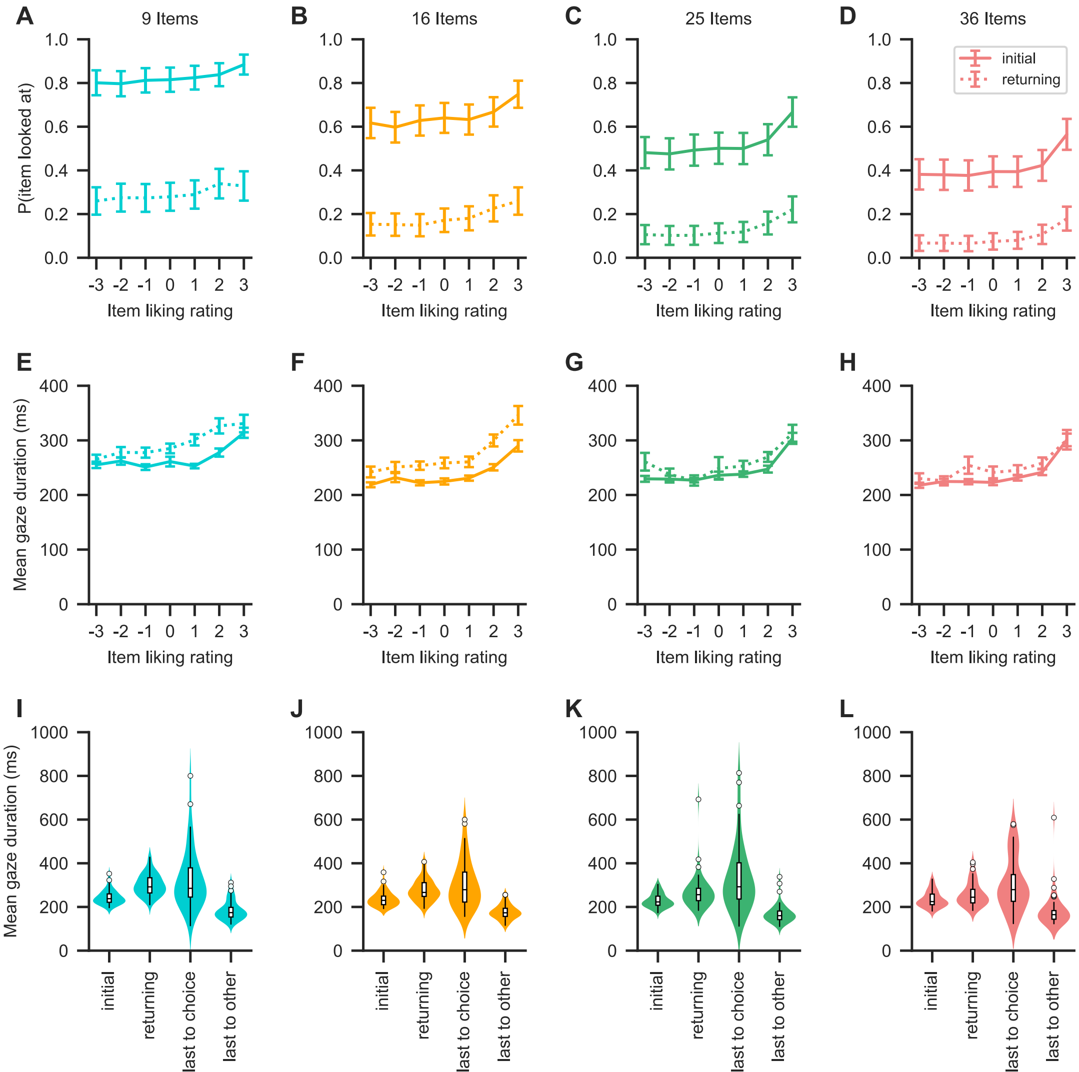

Figure 2: Gaze psychometrics for each choice set size. A-H: The probability of looking at an item (A-D) as well as the mean duration of item gazes (E-H) increases with the liking rating of the item. Solid lines indicate initial gazes to an item, while dotted lines indicate all subsequent returning gazes to the item. I-L: Initial gazes to an item are in general shorter in duration than all subsequent gazes to the same item in a trial. The last gaze of a trial is in general longer in duration if it is to the chosen item than when it is to any other item. See the "Visual Search" section for the corresponding statistical analyses. Colors indicate choice set sizes. Violin plots show a kernel density estimate of the distribution of subject means with boxplots inside of them.

To first establish a general understanding of the visual search process in MAFC, we performed an exploratory analysis of subjects' visual search behaviour (Figs. 2-3). We define a gaze to an item as all consecutive fixations towards the item that happen without any interrupting fixation to other parts of the choice screen. Further, we define the cumulative gaze of an item as the fraction of total trial time that the subject spent looking at the item (see “Methods”).

All reported regression coefficients represent fixed effects from mixed-effects linear (for continuous dependent variables) and logit (for binary dependent variables) regression models, which included random intercepts and slopes for each subject (unless noted otherwise). The 94% highest density intervals (HDI; 94% is the default in ArviZ 0.9.0 (Kumar, Carroll, Hartikainen & Martin, 2019) which we used for our analyses) of the fixed effect coefficients are given in brackets, unless noted otherwise (see “Methods”).

The probability that participants looked at an item in a choice set increased with the item’s liking rating, while decreasing with choice set size (Fig. 2 A-D; β = 2.0%, 94% HDI = [1.6, 2.3] per rating, -1.4%, 94% HDI = [-1.5, -1.3] per item) (in line with recent empirical findings: Cavanagh, Malalasekera, Miranda, Hunt, & Kennerley, 2019; Gluth et al., 2020). Similarly, the probability that participants’ gaze returned to an item also increased with the item’s rating while decreasing with choice set size (Fig. 2 A-D; β = 1.6%, 94% HDI = [1.4, 1.8] per rating, -0.65%, 94% HDI = [-0.74, -0.55] per item).

Gaze durations also increased with the item’s rating (Fig. 2 E-H; β = 11 ms, 94% HDI = [8, 13] per rating) as well as over the course of a trial (β = 0.79 ms, 94% HDI = [0.36, 1.25] per additional gaze in a trial), while decreasing with choice set size (β = -1.17 ms, 94% HDI = [-1.39, -0.94] per item). Initial gazes to an item were generally shorter in duration than all later gazes to the same item in the same trial (Fig. 2 I-L; β = 44 ms, 94% HDI = [37, 51] difference between returning and initial gazes). Interestingly, the duration of the last gaze in a trial was dependent on whether it was to the chosen item or not (Fig. 2 I-L): last gaze durations to the chosen item were in general longer than last gaze durations to non-chosen items (β = 162 ms, 94% HDI = [122, 201] difference between last gazes to chosen and non-chosen items).

Next, we focused on subjects’ visual search trajectories (Fig. 3): For each trial, we first normalized time to a range from 0 - 100% and then binned it into 10% intervals. We then extracted the liking rating, position, and size for each item in a trial (see “Methods”). An item’s position was encoded by its column and row indices in the square grid (see Fig. 1; with indices increasing from left to right and top to bottom). All item attributes were centered with respect to their trial mean in the choice set (e.g., a centered row index of -1 in the choice set size with 9 items represents the row one above the center, whereas a centered item rating of -1 represents a rating one below the average of all item ratings in that choice set). For each normalized time bin, we computed a mixed effects logit regression model (see "Methods"), regressing the probability that an item was looked at onto its attributes.

In general, subjects began their search at the center of the screen (Fig. 3 A-B; as indicated by regression coefficients close to 0 for the items' row and column positions in the beginning of a trial), coinciding with the preceding fixation cross. Subjects then typically transitioned to the top left corner (Fig. 3 A-B; as indicated by increasingly negative regression coefficients for the items' row and column positions in the beginning of a trial) and then moved from top to bottom (Fig. 3 B; as indicated by the then increasingly positive regression coefficients for the items' row positions). Over the course of the trial, subjects generally focused their search more on highly rated (Fig. 3 C) and larger (Fig. 3 D) items, while the probability that their gaze returned to an item also steadily increased (Fig. 3 E; $\beta = 9.9\%$, 94% HDI = [9.2, 10.7] per second, -0.73, 94% HDI = [-0.80, -0.66] per item), as did the durations of these gazes (Fig. 3 F; $\beta = 14$ ms, 94% HDI = [12, 17] per second, -2.9 ms, 94% HDI = [-3.3, -2.5] per item). In general, the effects of item position and size on the search process decreased over time (Fig. 3 A-B, D). For exemplar visual search trajectories in each set size condition, see Supplementary Files 1-4.

Overall, the fraction of total trial time that subjects looked at an item was dependent on the liking rating, size, and position of the item, as well as the number of items contained in the choice set ($\beta = 0.5\%$, 94% HDI = [0.4, 0.6] per liking rating, 0.02%, 94% HDI = [0.008, 0.03] per percentage increase in size, -0.20%, 94% HDI = [-0.24, -0.15] per row position, -0.044, 94% HDI =[-0.075, -0.007] per column position, -0.177, 94% HDI = [-0.18, -0.174] per item).

We also tested whether these item attributes influenced subjects' choice behaviour. However, the probability of choosing an item did not depend on the size or position of the item, but was solely dependent on the item's rating and the set size ($\beta = 3.88$, 94% HDI = [3.53, 4.26] per rating, 0.02, 94%

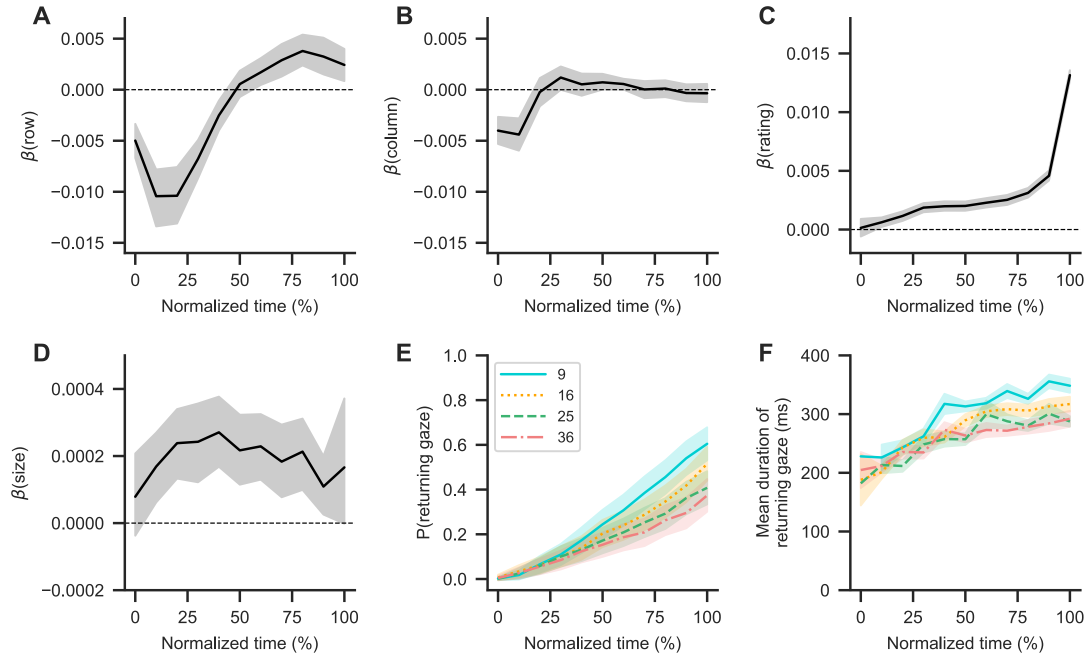

Figure 3. Visual search trajectory: A-D: Black lines represent the fixed effects coefficient estimates (with 94% HDI intervals surrounding them) of a mixed effects logit regression analysis (see "Methods") for each normalized trial time bin regressing the probability that an item was looked at onto its centered attributes (row (A) and column (B) position, liking rating (C), and size (D); see "Methods"). Subjects generally started their search in the center of the choice screen, coinciding with the fixation cross, and then transitioned to the top left corner (as indicated by decreasing regression coefficients for the items' row (A) and column positions (B)). From there, subjects generally searched from top to bottom (as indicated by slowly increasing regression coefficients for the items' row positions (A)), while also focusing more on items with a high liking rating (C) and a larger size (D). Dashed horizontal lines indicate a coefficient estimate of 0. E-F: Over the course over a trial, subjects were also more likely to look at items that they had already seen in the trial (E), while the duration of these returning gazes also increased (F). See the "Visual Search" section for details on the corresponding statistical analyses. Lines indicate mean values with standard errors surrounding them. Colors and line styles in E-F represent choice set size conditions.

HDI = [-0.015, 0.06] per percentage increase in item size, -0.06, 94% HDI = [-0.12, 0.01] per row, -0.03, 94% HDI = [-0.1, 0.03] per column, -0.24, 94% HDI = [-0.25, -0.23] per item).

Competing choice models

We consider the following set of decision models, spanning the space between rational choice and gaze-driven evidence accumulation.

The optimal choice model with zero search costs is based on the framework of rational decision-making (Luce & Raiffa, 1957; Simon, 1955). It assumes that individuals look at all the items of a choice set and then choose the best seen item with a fixed probability β, while making a probabilistic choice over the set of seen items with probability *1*-β following a softmax choice rule based on the items' values (*l)*:

$\sigma_i = \frac{exp(\tau \times l_i)}{\sum_j exp(\tau \times l_j)}$.

The hard satisficing model assumes that individuals search until they either find an item with reservation value *V* or higher, or they have looked at all items (Caplin et al., 2011; Fellows, 2006; McCall, 1970; Payne, 1976; Schwartz et al, 2002; Simon, 1955, 1956, 1957, 1959; Stüttgen et al, 2012). In the former case, individuals immediately stop their search and choose the first item that meets the reservation value. Crucially, the reservation value can vary across individuals and set-size conditions. In the latter case, individuals make a probabilistic choice over the set of seen items, as in the optimal choice model.

Based on the findings by Reutskaja and colleagues (2011), we also considered a probabilistic version of satisficing, which combines elements from the optimal choice and hard satisficing models. Specifically, the probabilistic satisficing model (PSM) assumes that the probability *q(t)* with which individuals stop their search and make a choice at time point *t* increases with elapsed time in the trial and the cached (i.e., highest-seen) item value. Once the search ends, individuals make a probabilistic choice over the set of seen items, as in the other two models (see "Methods").

Next, we considered an independent evidence accumulation model (IAM), in which evidence for an item begins accumulating once the item is looked at (Smith & Vickers 1988). Importantly, each accumulator evolves independently from the others, based on the subjective value of the represented item.

Once the accumulated evidence for an alternative reaches a predefined decision threshold, a choice is made for that alternative (much like deciding whether the item satisfies a reservation value) (see “Methods”).

In line with many empirical findings (e.g., Krajbich et al., 2010, 2011; Lopez-Persem, et al., 2017; Tavares et al., 2017; Smith & Krajbich 2019; Thomas et al., 2019), we also considered a relative evidence accumulation model (as captured by the gaze-weighted linear accumulator model (GLAM); Thomas et al., 2019; Molter, Thomas, Heekeren & Mohr 2019), which assumes that individuals accumulate and compare noisy evidence in favor of each item relative to the others. As with the independent accumulation model, a choice is made as soon as the accumulated relative evidence for an item reaches a predetermined decision threshold (see “Methods”).

We further considered two different accounts of gaze in the decision process. The passive account of gaze assumes that gaze allocation solely determines the set of items that are being considered; an item is only considered once it is looked at. In contrast, the active account of gaze assumes that gaze influences the subjective value of an item in the decision process, thereby generating higher choice probabilities for items that are looked at longer. In the PSM, the subjective value of each item increases with gaze time. Similarly, in the accumulator models, the accumulation rate for an item (indicating subjective value) increases when it is being looked at.

Recent empirical findings indicate two distinct mechanisms through which gaze might actively influence these decision processes: multiplicative effects (Krajbich et al., 2010, 2011; Lopez-Persem, et al., 2017; Tavares et al., 2017; Smith & Krajbich 2019; Thomas et al., 2019) and additive effects (Cavanagh et al., 2014; Westbrook et al. 2020). Multiplicative effects discount the subjective values of unattended items (by multiplying them with $\gamma; 0 \leq \gamma \leq 1$), while additive effects add a constant boost ($\zeta; 0 \leq \zeta \leq 10$) to the subjective value of the attended item. Thus, multiplicative effects are proportional to the values of the items, while additive effects are constant for all items. We allow for both of these mechanisms in the modeling of the active influence of gaze on the decision process (see “Methods”).

Qualitative model comparison

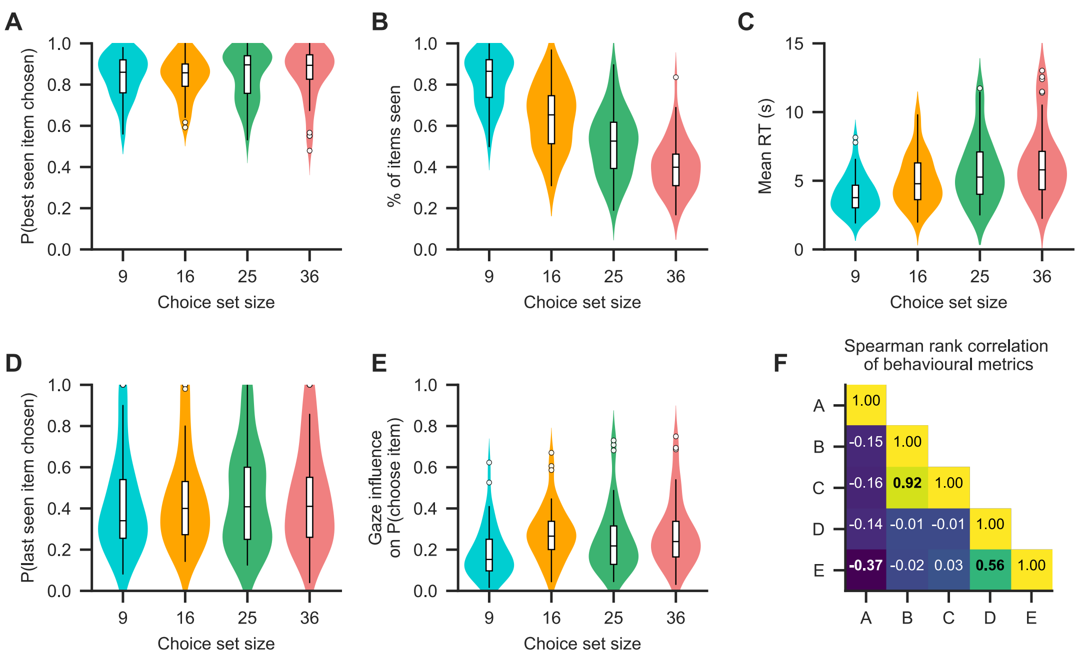

Figure 4. Choice psychometrics for each choice set size. A: The subjects were very likely to choose one of the highest-rated (i.e., best) items that they looked in all choice set sizes. B-C: The fraction of items of a choice set that subjects looked at in a trial decreased with choice set size (B), while subjects' mean RTs increased (C). D: Subjects chose the item that they looked at last in a trial about half the time. E: Subjects generally exhibited a positive association of gaze allocation and choice behaviour (as indicated by the gaze influence measure, describing the mean increase in choice probability for an item that is looked at longer than the others, after correcting for the influence of item value on choice probability; for details on this measure, see "Qualitative model comparison"). F: Associations of the behavioural measures shown in panels A - E (as indicated by Spearman's rank correlation due to non-normal distributions of pooled subject means). Correlations are computed by the use of the pooled subject means across the choice set size conditions. Correlations with P-values smaller than 0.01 (Bonferroni corrected for multiple comparisons: 0.1/10) are printed in bold font. For a detailed overview of the associations of the behavioural measures, see Figure 4-figure supplement 1. See the "Qualitative model comparison" section for the corresponding statistical analyses. For a detailed overview of the associations between the behavioural choice measures and individuals' visual search, see Figure 4-figure supplement 2. Different colors in A-E represent the choice set size conditions. Violin plots show a kernel density estimate of the distribution of subject means with boxplots inside of them.

First, we probed the assumptions of the optimal choice model with zero search costs, which predicts that subjects first look at all the items in a choice and then choose the highest-rated item at a fixed rate. Conditional on the set of looked-at items, subjects chose the highest-rated item at a very consistent rate across set sizes (Fig. 4 A; $\beta = 0.05\%$, 94% HDI = [-0.04,0.14] per item), with an overall average of 84%. However, subjects did not look at all food items in a given trial (Fig. 4 B), while the fraction of items in a choice set that subjects looked at decreased across set sizes (Fig. 4 B; β = -1.5%, 94% HDI = [-1.6, -1.4] per item) and their RTs increased (Fig. 4 C; β = 85 ms, 94% HDI = [67, 102] per item). This immediately ruled out a strict interpretation of the optimal choice model, as subjects did not look at all items before making a choice.

Next, we tested the assumptions of the hard satisficing model, which predicts that subjects should stop their search and make a choice as soon as they find an item that meets their acceptance threshold. Accordingly, the last item that subjects look at should be the one that they choose (unless they look at every item). However, across choice set sizes, subjects only chose the last item that they looked at in 44.5% of the trials (Fig. 4 D; β = 0.13%, 94% HDI = [-0.001, 0.26] per item). Even within the trials where subjects did not look at every item, the probability that they chose the last seen item was on average only 44.1%.

The PSM, on the other hand, predicts that the probability with which subjects stop their search and make a choice increases with elapsed time and cached value (i.e., the highest-rated item seen so far in a trial). We found that both had positive effects on subjects' stopping probability, in addition to a negative effect of choice set size (β = 2.7%, 94% HDI = [2.0, 3.3] per cached value, 2.26%, 94% HDI = [1.69, 2.80] per second, -0.22%, 94% HDI = [-0.24, -0.20] per item). Subjects' behaviour was therefore qualitatively in line with the basic assumptions of the PSM. Note that this finding does not allow us to discriminate between the PSM and evidence accumulation models, because both make very similar qualitative predictions about the relationship between stopping probability, time, and item value.

Lastly, we probed individuals' behavioural association of gaze allocation and choice. To this end, we utilized a previously proposed measure of gaze influence (Krajbich et al, 2010, 2011; Thomas et al., 2019): First, we regressed a choice variable (1 if the item was chosen, 0 otherwise) on the relative liking rating of each item in the choice set (the difference between the item's rating and the mean rating of all other items in that set) as well as the mean and range of the other items' liking ratings. This model estimates the probability of choosing each of the items based purely on the items' liking ratings. We then subtracted the resulting estimated choice probability for each item in each trial from the empirically observed choice for this item. Finally, we aggregated the resulting residual choice probabilities for all positive and negative cumulative gaze advantages (describing whether an item was looked at longer than the others over the course of the trial or not) and computed the difference between the two.

We found that all subjects exhibited positive values on this measure in all set sizes (Fig. 4 E; with values ranging from 1.7% to 75%) and that it increased with choice set size (Fig. 4 E; $\beta = 0.26\%$, 94% HDI = [0.15, 0.39] per item), indicating an overall positive association between gaze allocation and choice. In general, a subject's probability of choosing an item increased with the item's cumulative gaze advantage (defined as the difference between the item's cumulative gaze and the maximum cumulative gaze of all other items in a choice set) and the item's relative rating, while it decreased with the range of the ratings of the other items in a choice set and choice set size ($\beta = 0.46\%$, 94% HDI = [0.4, 0.5] per percentage increase in gaze advantage, 3.6%, 94% HDI = [3.2, 4.0] per unit increase in relative rating, -2.8%, 94% HDI = [-3.1, -2.4] per unit increase in the range of ratings of the other items, -0.16, 94% HDI = [-0.18, -0.14] per item).

To further probe the assumption of gaze-driven evidence accumulation, we performed three tests: According to the framework of gaze-driven evidence accumulation, subjects who exhibit a stronger association between gaze and choice should generally exhibit a lower probability of choosing the highest-rated item from a choice set (for a detailed discussion on this finding, see Thomas et al., 2019). For these subjects, the gaze bias mechanism can bias the decision process towards items that have a lower value but were looked at longer. In line with this prediction, we found that probability of choosing the highest-rated seen item was negatively correlated with the gaze influence measure ($\beta = -0.22\%$, 94% HDI = [-0.36, -0.08] per percentage increase in gaze influence; the mixed effects regression included a random slope and intercept for each set size).

Second, subjects who have a stronger association between gaze and choice should also be more likely to choose the last-seen item, as evidence for the looked-at item is accumulated at a generally higher rate. In line with this prediction, subjects with a stronger relation between gaze and choice were generally also more likely to choose the item that they looked at last (β = 1.1%, 94% HDI = [0.9, 1.3] per percentage increase in gaze influence; the mixed effects regression included a random slope and intercept for each set size).

Last, subjects who exhibit a positive association between gaze and choice should be more likely to choose an item when it receives longer individual gazes. In line with previous work (e.g., Krajbich et al., 2010, 2011), we investigated this by studying the probability of choosing the first-seen item as a function of the first gaze duration. Overall, this relationship was positive (as was the influence of the item's rating), while decreasing with choice set size (β = 17.81%, 94% HDI = [13.72, 22.22] per second, 6.0%, 94% HDI = [5.5, 6.6] per rating, -0.27%, 94% HDI = [-0.32, -0.22] per item).

Relation of visual search and choice behaviour

To better understand the relationship between visual search and choice behavior, we also studied the association of the influence of an item's size, rating, and position on gaze allocation with the metrics of choice behavior reported in Fig. 4 (namely, mean RT, fraction of looked-at items, probability of choosing the highest-rated seen item, and gaze influence on choice) (see Figure 4-figure supplement 2). To quantify the influence of the item attributes on gaze allocation, we ran a regression for each subject of cumulative gaze (defined as the fraction of trial time that the subject looked at an item; scaled 0 - 100 %) onto the four item attributes (row, column, size, and rating) and choice set size, resulting in one coefficient estimate (β_{gaze}) for the influence of each of the item attributes and choice set size on cumulative gaze.

Subjects with a stronger influence of rating on gaze allocation generally looked at fewer items (β = -17%, 94% HPI = [-31, -4] per unit increase in β_{gaze}(rating); Figure 4-figure supplement 2 H), were more likely to choose the highest-rated seen item (β = 14%, 94% HDI = [4, 23] per unit increase in β_{gaze}(rating); Figure 4-figure supplement 2 P), and were more likely to choose the last seen item (β = 41%, 94% HDI = [20, 63] per unit increase in β_{gaze}(rating); Figure 4-figure supplement 2 T). Subjects with a stronger influence of item size on gaze allocation generally looked at fewer items (β = -114%, 94% HDI = [-217, -8] per unit increase in β_{gaze}(size); Figure 4-figure supplement 2 G), exhibited shorter RTs (β = -18 s, 94% HDI = [-33, -4] per unit increase in β_{gaze}(size); Figure 4-figure supplement 2 K), and were less likely to choose the last seen item (β = -196%, 94% HDI = [-359, -40] per unit increase in β_{gaze}(size); Figure 4-figure supplement 2 S). Lastly, subjects with a stronger influence of column number (horizontal location) on gaze allocation generally exhibited longer RTs (β = 3.9 s, 94% HDI = [0.1, 7.8] per unit increase in β_{gaze}(column); Figure 4-figure supplement 2 J). We did not find any other statistically meaningful associations between visual search and choice metrics (see Figure 4-figure supplement 2).

Quantitative model comparison

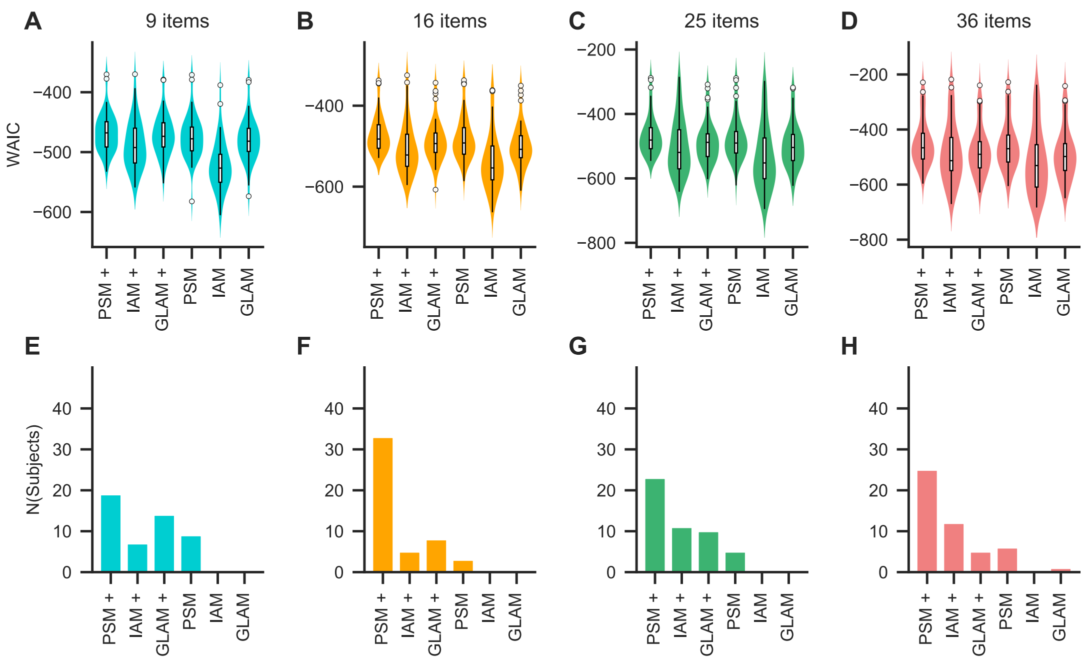

Figure 5. Relative model fit. A-D: Individual WAIC values for the probabilistic satisficing model (PSM), independent evidence accumulation model (IAM), and gaze-weighted linear accumulator model (GLAM) for each set size. Model variants with an active influence of gaze are marked with an additional ”+”. The WAIC is based on the log-score of the expected pointwise predictive density such that larger values in WAIC indicate better model fit. Violin plots show a kernel density estimate of the distribution of individual values with boxplots inside of them. E-H: Number of subjects for each set size that were best described by each of the model variants. For an overview of the distribution of individual model parameter estimates, see Figure 5-figure supplement 1 and Supplementary Files 5-7. For an overview of the results of a model recovery of the three model types, see Figure 5-figure supplement 2. Colors indicate choice set sizes.

Taken together, our findings have shown that subjects’ choice behaviour in MAFC does not match the assumptions of optimal choice or hard satisficing, while it qualitatively matches the assumptions of probabilistic satisficing and gaze-driven evidence accumulation. To further discriminate between the evidence accumulation and probabilistic satisficing models, we fitted them to each subject’s choice and RT data for each set size (see “Methods”; for an overview of the parameter estimates, see Figure 5-figure supplement 1and Supplementary Files 5-7). and compared their fit by means of the Widely Applicable Information Criterion (WAIC; Vehtari, Gelman, & Gabry, 2017). Importantly, we tested two variants of each of these models, one with a passive account of gaze in which gaze allocation

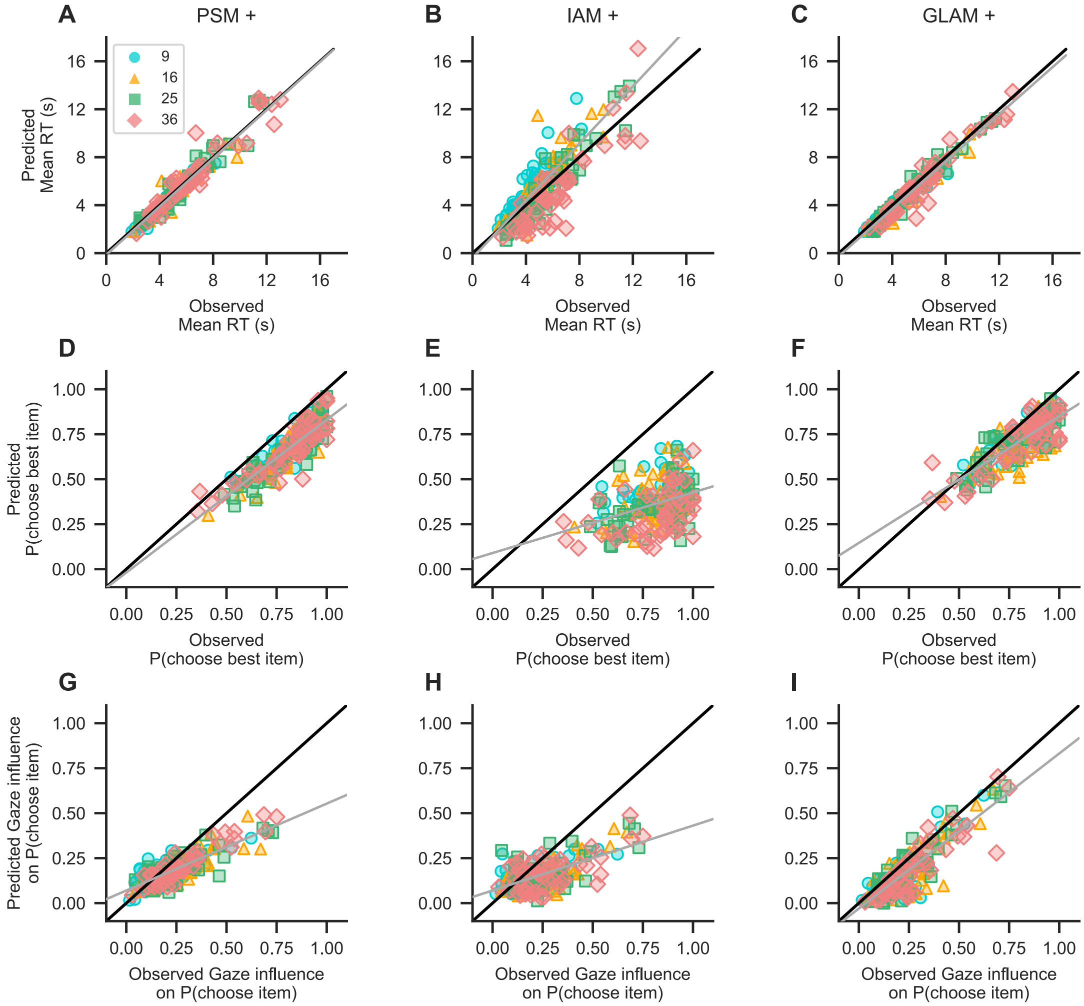

Figure 6. Absolute model fit. Predictions of mean RT (A-C), probability of choosing the highest-rated (i.e., best) seen item (D-F), and gaze influence on choice probability (G-I; for details on this measure, see "Qualitative model comparison") by the active-gaze variants of the probabilistic satisficing model (PSM+; A, G, D), independent evidence accumulation model (IAM+; B, E, H), and gaze-weighted linear accumulator model (GLAM+; C, F, I). A-C: The PSM+ and GLAM+ accurately recover mean RT, which the IAM+ accurately but imprecisely recovers. D-F: The PSM+ provides the overall best account of choice accuracy, followed by the GLAM+, and IAM+. G-I: The PSM+ and IAM+ clearly underestimate strong influences of gaze on choice; the GLAM+ provides the best account of this association and only slightly underestimates strong influences of gaze on choice. Gray lines indicate mixed-effects regression fits of the model predictions (including a random intercept and slope for each set size) and black diagonal lines represent ideal model fit. Model predictions are simulated using parameter estimates obtained from individual model fits (for details on the fitting and simulation procedures, see "Methods"). See the "Quantitative model comparison" section for the corresponding statistical analyses. Colors/shapes represent different set sizes, while points indicate individual subjects.

solely determines the set of items that are considered in the decision process, and the other with an active account of gaze in which gaze affects the subjective value of the alternatives. In the active-gaze models (as indicated by the addition of a "+" to the model name), we allowed for both multiplicative and additive effects of gaze on the decision process (see "Methods"). The model variants with a passive and active account of gaze were identical, other than for these two influences of gaze on subjective value. Note that all three model types can be recovered to a satisfying degree in our data (see Figure 5-figure supplement 2).

According to the WAIC, the choice behaviour of the majority of subjects in all set size conditions was best described by the PSM+ (Fig. 5; 39% (19/49), 67% (33/49), 47% (23/49), and 51% (25/49) in the sets with 9, 16, 25, and 36 items respectively). The model that best explained the remaining subjects was the GLAM+ for 9 and 16 items (Fig. 5; 29% (14/49) and 16% (8/49) subjects respectively), and the IAM+ for 25 and 36 items (Fig. 5; 22% (11/49) and 24% (12/49) subjects respectively). Overall, the vast majority of subjects were best captured by the model variants with an active account of gaze (82% (40/49), 94% (46/49), 90% (44/49), and 86% (42/49) for 9, 16, 25, and 36 items respectively).

To also probe the ability of these models to capture choice behaviour on an absolute level, we simulated choice and RT data for each subject with the three active-gaze models (Fig. 6; see "Methods"). We assessed the quality of the simulations by regressing the predicted mean RT, probability of choosing the highest-rated item, and gaze influence on choice probability onto the observed subject values for each of these measures, in a linear mixed-effects regression analysis with one random intercept and slope for each set size (see "Methods"). If a model captures the data well, the resulting fixed effects regression line should have an intercept of 0 and a slope of 1 (as indicated by the black diagonal lines in Fig. 6).

The PSM+ and GLAM+ both accurately recovered mean RT (Fig. 6 A, C; intercept = -138 ms, 94% HDI = [-414, 119], β = 1.01 ms, 94% HDI = [0.95, 1.05] per ms increase in observed RT for the PSM+; intercept = -247 ms, 94% HDI = [-499, 11], β = 0.98 ms, 94% HDI = [0.94, 1.03] per ms increase in observed RT for the GLAM+), which the IAM+ accurately, but imprecisely, recovered (Fig. 6 B; intercept = -397 ms, 94% HDI = [-1764, 1331], β = 1.19 ms, 94% HDI = [0.96, 1.43] per ms increase in observed RT). All three models generally underestimated high probabilities of choosing the highest-rated item from a choice set (Fig. 6 D-F), while the PSM+ provided the overall most accurate account of this metric (Fig. 6 D; intercept = -1.90%, 94% HDI = [-7.64, 3.19], β = 0.85%, 94% HDI = [0.79, 0.91] per percentage increase in observed probability of choosing the highest-rated item), followed by the GLAM+ (Fig. 6 E; intercept = 14.55%, 94% HDI = [8.08, 21.21], β = 0.70%, 94% HDI = [0.62, 0.77] per percentage increase in observed probability of choosing the highest-rated item), and IAM+ (Fig. 6 F; intercept = 8.95%, 94% HDI = [-2.76, 26.17], β = 0.34%, 94% HDI = [0.21, 0.46] per percentage increase in observed probability of choosing the highest-rated item).

Turning to the gaze data, the PSM+ and IAM+ both slightly overestimated weak associations between gaze and choice while clearly underestimating stronger associations between them (Fig. 6 G-H; intercept = 7.03%, 94% HDI = [4.95, 10.23], β = 0.48%, 94% HDI = [0.38, 0.56] per percentage increase in observed gaze influence for the PSM+; intercept = 7.03%, 94% HDI = [4.57, 9.37], β = 0.36%, 94% HDI = [0.29, 0.44] per percentage increase in observed gaze influence for the IAM+). The GLAM+, in contrast, only slightly underestimated the association between gaze and choice (Fig. 6 I; intercept = -3.01%, 94% HDI = [-5.79, -0.22], β = 0.86%, 94% HDI = [0.76, 0.96] per percentage increase in observed gaze influence).

Discussion

The goal of this work was to identify the computational mechanisms underlying choice behaviour in MAFC, by comparing a set of decision models on choice, RT, and gaze data. In particular, we tested models of optimal and satisficing choice (Reutskaja et al., 2011; Caplin et al., 2011; Fellows, 2006; Fellner et al., 2009; McCall, 1970; Payne, 1976; Schwartz et al., 2002; Stüttgen et al., 2012) as well as relative (Krajbich & Rangel, 2011; Thomas et al., 2019) and independent evidence accumulation (Smith & Vickers 1988). We further tested two variants of these models, with and without influences of gaze on subjective value. We found that subjects' behaviour qualitatively could not be explained by optimal choice or standard instantiations of satisficing. After incorporating active effects of gaze into a probabilistic version of satisficing, it explained the data well, outperforming the evidence accumulation models in fitting choice and RT data. Still, the relative accumulation model provided by far the best fit to the observed association between gaze allocation and choice behaviour, which was not explicitly accounted for in the likelihood-based model comparison.

The active-gaze satisficing model performed comparably well to the relative accumulation model for the smallest set size (with 9 alternatives), but stood apart for the larger set sizes (16, 25, and 36 alternatives). The relative accumulation model also steadily performed worse compared to the independent accumulation model as set size increased. Together, these results suggest that relative evidence accumulation is a less plausible choice mechanism as the number of alternatives increases, at least in its current formulation. Intuitively this makes sense, since the number of comparisons explodes as the number of alternatives grows; for 36 alternatives there are up to 630 potential comparisons. Meanwhile, the number of decision processes in the independent accumulator model only grows linearly with the number of seen alternatives.

One reason why the satisficing model might perform particularly well for large sets, is that in our experiment there were a limited number of food items (80; see "Methods"). Each item was repeated an average of 50 times per experiment. Thus, subjects could have learned to search for specific items. In practice, this strategy would only be useful in certain scenarios. At your local vending machine, you are almost guaranteed to encounter one of your favorite snacks; here satisficing would be useful. But at a foreign vending machine, or a new restaurant, the evidence accumulation framework might be more useful. Future work is needed to investigate the performance of these models in novel and familiar choice environments.

These findings are also relevant to the discussion about the direction of causality between attention and choice. Several papers have argued that subjective value and/or the emerging choice affect gaze allocation, both in binary choice (Cavanagh et al., 2014; Westbrook et al., 2020) and in multi-alternative choice (Krajbich & Rangel, 2011; Towal et al., 2013; Gluth et al., 2020; Callaway et al., 2020). Other work has argued that gaze drives choice outcomes, using exogenous manipulations of attention (Armel et al. 2008; Mormann et al. 2012; Parnamets et al. 2015; Tavares et al. 2017; Gwinn et al,. 2019, c.f. Newell & LePelley, 2018; Ghaffari & Fiedler, 2018). Here, we find support for both directions of the association of gaze and choice. In contrast to the binary choice setting (Krajbich et al. 2010), we found that the probability that an item was looked at, as well as the duration of a gaze to this item, increased with the item's rating, and that this trend also increased over the course of a trial. Nevertheless, our data also indicates that gaze affects choice above and beyond the values of the items (Fig. 4 E-F).

In a sense the contrast between binary and multi-alternative choice is not surprising. When deciding between two alternatives, you are merely trying to compare one to the other. In that case attending to either alternative is equally useful in reaching the correct decision. However, with many choice alternatives, it is in your best interest to quickly identify the best alternatives in the choice set and exclude all other alternatives from further consideration (e.g. Hauser & Wernerfelt, 1990; Payne, 1976; Reutskaja et al., 2011; Roberts & Lattin, 1991). Given this search and decision process we might expect that subjects' choices are more driven by their gaze in the later stages of the decision, when they focus more on the highly rated items in the choice set, than in the earlier stages of the search, when gaze is driven by the items' positions and sizes. Indeed, we found that only the items' ratings predicted choice behaviour, not their positions or sizes.

As in prior work, our findings firmly reject a model of complete search and maximization in MAFC (Caplin et al., 2011; Pieters & Warlop, 1999; Reutskaja et al., 2011; Simon, 1959; Stüttgen et al., 2012): Subjects do not look at every item and they do not always choose the best item they have seen. Our data also clearly reject the hard satisficing model: Subjects choose the last item they look at only half of the time. Additionally, we find that subjects' choices are strongly dependent on the actual time that they spent looking at each alternative and can therefore not be fully explained by simply accounting for the set of examined items. This stands in stark contrast to many models of consumer search and rational inattention (e.g., Caplin, Dean & Leahy, 2019; Masatlioglu, Nakajima & Ozbay, 2012; Matějka & McKay, 2015; Sims, 2003), which ascribe a more passive role to visual attention, by viewing it as a filter that creates consideration sets (by attending only to a subset of the available alternatives) from which the decision maker then chooses. Our findings indicate that attention takes a much more active role in MAFC by guiding preference formation within the consideration set, as has been observed with smaller choice sets (e.g., Armel et al., 2008; Gluth et al., 2020; Krajbich et al., 2010, 2011; Smith & Krajbich, 2019; Thomas et al., 2019).

In conclusion, we find that models of gaze-weighted subjective value account for relations between eye-tracking data and choice that other passive-attention models of MAFC cannot. These findings provide new insight into the mechanisms underlying search and choice behaviour, and demonstrate the importance of employing choice-process techniques and computational models for studying decision-making.

Materials and methods

Experimental design

49 healthy English speakers completed this experiment (17 female; 18-55 yrs, median: 23 yrs). All subjects were required to have normal or corrected-to-normal vision. Individuals wearing glasses or hard contact lenses were excluded from this study. Further, individuals were only allowed to participate, if they self-reportedly (I) fasted at least four hours prior to the experiment, (II) regularly ate the snack foods that were used in the experiment, (III) neither had any dietary restrictions nor (IV) a history of eating disorders, and (V) didn't diet within the last six months prior to the experiment. The sample size for this experiment was determined based on related empirical research at the time of data collection (e.g., Berkowitsch et al., 2014; Cavanagh et al., 2014; Krajbich et al., 2010, 2011; Philiastides & Ratcliff, 2013; Reutskaja et al., 2011; Rodriguez et al., 2014; Towal et al., 2013). Informed consent was obtained from all subjects in a manner approved by the Human Subjects Internal Review Board (IRB) of the California Institute of Technology (IRB protocol: "Behavioural, eye-tracking, and psychological studies of simple decision-making"). Each subject completed the following tasks within a single session: First, they did some training with the choice task, followed by the choice task (Fig. 1), a liking rating task, and the choice implementation.

In the choice task (Fig. 1), subjects were instructed to choose the snack food item that they would like to eat most at the end of the experiment from sets of 9, 16, 25, or 36 alternatives. There was no time restriction on the choice phase and subjects indicated the time point of choice by pressing the space bar of a keyboard in front of them. After pressing the space bar, subjects had 3 seconds to indicate their choice with the mouse cursor (for an overview of the choice indication times, defined as the time difference between the space bar press and the click on an item image, see Figure 1-figure supplement 1). Subjects used the same hand to press the space bar and navigate the mouse cursor. If they did not choose in time, the choice screen disappeared and the trial was marked invalid and excluded from the analysis as well as the choice implementation. We further excluded trials from the analysis if subjects either chose an item that they didn't look at before pressing the spacebar, or if they clicked on the empty space between item images. The average number of trials dropped from the analysis was 3 (SE: 0.5) per subject and set size condition.

The initial training task had the exact same structure as the main choice task and differed only in the number of trials (5 trials per set size condition) and the stimuli that were used (we used a distinct set of 36 snack food item images).

In the subsequent rating task, subjects indicated for each of the 80 snack foods, how much they would like to eat the item at the end of the experiment. Subjects entered their ratings on a 7-point rating scale, ranging from -3 (not at all) to +3 (very much), with 0 denoting indifference (for an overview of the liking rating distributions, see Figure 1-figure supplement 2-3).

After the rating task, subjects stayed for another 10 minutes and were asked to eat a single snack food item, which was selected randomly from one of their choices in the main choice task. In addition to one snack food item, subjects received a show-up fee of $10 and another $15 if they fully completed the experiment.

Experimental stimuli

The choice sets of this experiment were composed of 9, 16, 25, or 36 randomly selected snack food item images (random selection without replacement within a choice set). For each set size condition, these images were arranged in a square matrix shape, with the same number of images per row and column (3, 4, 5, or 6). All images were displayed in the same size and resolution (205 x 133 px) and depicted a single snack food item centered in front of a consistent black background.

During the rating phase single item images were presented one at a time and in their original resolution (576 x 432 px), again centered in front of a consistent black background (see Fig. 1). Overall, we used a set of 80 different snack food items for the choice task and a distinct set of 36 items for the training.

Eye tracking

Monocular eye tracking data were collected with a remote EyeLink 1000 system (SR Research Ltd., Mississauga, Ontario, Canada) with a sampling frequency of 500 Hz. Before the start of each trial, subjects had to fixate a central fixation cross for at least 500 ms to ensure that they began each trial fixating on the same location (see Fig. 1).

Eye tracking measures were only collected during the choice task and always sampled from the subject's dominant eye (10 left-dominant subjects). Stimuli were presented on a 19-inch LCD display with a resolution of 1280 x 1024 px. Subjects had a viewing distance of about 50 cm to the eye tracker and 65 cm to the display. Several precautions were taken to ensure a stable and accurate eye tracking measurement throughout the experiment, as we presented up to 36 items on a single screen: (I) the eye tracker was calibrated with a 13-point calibration procedure of the EyeLink system, which also covers the screen corners, (II) four separate calibrations were run throughout the experiment: once before and after the training task and twice during the main choice task (after 75 and 150 trials), (III) subjects placed their head on a chin rest, while we recorded their eye movements.

Fixation data were extracted from the output files obtained by the EyeLink software package (SR Research Ltd., Mississauga, Ontario, Canada). We used these data to define whether the subject's gaze was either within a rectangular region of interest (ROI) surrounding an item (item gaze), somewhere else on the screen (non-item gaze) or whether the gaze was not recorded at all (missing gaze, e.g., eye blinks). All non-item and missing gazes occurring before the first and after the last gaze to an item in a trial were discarded from all gaze analyses. All missing data that occurred between gazes to the same item were changed to that item and thereby included in the analysis. A gaze pattern of 'item 1, missing data, item 1' would therefore be changed to 'item 1, item 1, item 1'. Non-item or missing gaze times that occurred between gazes to different items, however, were discarded from all gaze analyses.

Item attributes

Liking rating

An item's liking rating (or value) is defined by the rating that the subject assigned to this item in the liking rating task (see Fig. 1).

Position

This metric described the position of an item in a choice set and was encoded by two integer numbers: one indicating the row in which the item was located and the other indicating the respective column. Row and column indices ranged between 1 and the square root of the set size (as choice sets had a square shape, with the same number of rows and columns; see Fig. 1). Importantly, indices increased from left to right and top to bottom. For instance, in a choice set with 9 items, the column indices would be 1, 2, 3, increasing from left to right, while the row indices would also be 1, 2, 3, but increase from top to bottom. The item in the top left corner of a screen would therefore have a row and column index of 1, whereas the item in the top right corner would have a row index of 1 and a column index of 3.

Size

This metric describes the size of an item depiction with respect to the size of its image. In order to compute this statistic, we made use of the fact that all item images had the exact same absolute size and resolution. First, we computed the fraction of the item image that was covered by the consistent black background. Subsequently, we subtracted this number from 1 to get a percentage estimate of how much image space is covered by the snack food item. As all item images had the same size and resolution, these percentage estimates are comparable across images.

Probabilistic satisficing model (PSM)

Our formulation of the probabilistic satisficing model (PSM) is based on a proposal by Reutskaja et al. (2011) and consists of two distinct components: a probabilistic stopping rule, defining the probability $q(t)$ with which the search ends and a choice is made at each time point *t* ($\Delta t = 1ms$), and a probabilistic choice rule, defining a choice probability λ_i for each item *i* in the choice set. Reutskaja et al. (2011) defined the stopping probability $q(t)$ as:

$$q(t) = min\{\alpha \times C(t) + v \times t, 1\} \text{ with } q(0) = 0, C(t) > 0, \{t, \alpha, v\} \geq 0 \quad (1)$$

Importantly, $q(t)$ increases linearly with the cached item value $C(t)$ and the trial time *t*. Note that we extend the original formulation of the model by Reutskaja and colleagues (2011) upon an active influence of gaze on the decision process. Specifically, we defined the cached item value as:

$$C(t) = max_J\left(c_j(t)\right) \quad (2)$$

$$c_i(t) = g_i(t) \times (l_i + \zeta) + \left(1 - g_i(t)\right) \times \gamma \times l_i \quad (3)$$

Here, $g_i(t)$ represents the fraction of elapsed trial time *t* that item *i* was looked at, while γ $(0 \leq \gamma \leq 1)$ and ζ $(0 \leq \zeta \leq 10)$ implement the multiplicative and additive gaze bias effects. While an item *i* is looked at, its value l_i (as indicated by the item's liking rating) is increased by ζ, whereas the value of all other items that are momentarily not looked at is discounted by γ. Note that we set $c_i(t) = 0$ for all items that were not yet looked at by time point *t*. To further ensure $C(t) > 0$ we re-scaled all liking ratings to a range from 1 to 7. The strength of the influence of $C(t)$ and *t* on $q(t)$ is determined by the two positive linear weighting parameters α and v. Note that $q(t)$ is bounded to $(0 \leq q(t) \leq 1)$. To obtain the passive-gaze variant of the PSM, we set $\gamma = 1$and $\zeta = 0$.

However, $q(t)$ does not account for the probability that the search has ended at any time point prior to *t*. In order to apply and fit the model to RT data, we need to compute the joint probability $f(t)$ that the search has not stopped prior to *t* and the probability that the search ends at time point *t*. Therefore, we correct $q(t)$ for the probability $Q(t)$ that the search has not stopped at any time point prior to *t*:

$$f(t) = q(t) \times Q(t-1) \quad (4)$$

$$Q(t) = \prod_1^t \left(1 - q(t)\right) \quad (5)$$

Once the search has ended, the model makes a probabilistic choice over the set of alternatives *J* following a softmax function of their cached values $c_i(t)$ (with scaling parameter τ):

$$\sigma_i(t) = \frac{exp(\tau \times c_i(t))}{\sum_J exp\left(\tau \times c_j(t)\right)} \quad (6)$$

Lastly, by multiplying the stopping probability $f(t)$ by $\sigma_i(t)$, we obtain the probability $p_i(t)$ that item *i* is chosen at time point *t*:

$$p_i(t) = f(t) \times \sigma_i(t) \quad (7)$$

Independent evidence accumulation model (IAM)

The independent evidence accumulation (IAM) model assumes that the choices follow an evidence accumulation process, in which evidence for an item is only accumulated once it was looked at in a trial and is then independent of all other items in a choice set (much like deciding whether the item satisfies a reservation value) (Smith & Vickers 1988). A choice is determined by the first accumulator that reaches a common pre-defined decision boundary *b,* which we set to 1. Specifically, the evidence accumulation process is guided by a set of decision signals D_i for each item *i* that was looked at in the trial:

$$D_i = g_i \times (l_i + \zeta) + (1 - g_i) \times \gamma \times l_i \quad (8)$$

Here, l_i indicates the item's liking rating, while g_i indicates the fraction of the remaining trial time (after time point $t0_i$ at which item *i* was first looked at in the trial) that the individual spent looking at item *i*. As in the PSM (see eq. 3), γ $(0 \leq q(t) \leq 1)$ and ζ $(0 \leq \zeta \leq 10)$ implement the multiplicative and additive gaze bias effects. To obtain the passive-gaze variant of the IAM, we set $\gamma = 1$and $\zeta = 0$.

At each time step *t* (with Δt = 1ms), the amount of accumulated evidence E_i is determined by a velocity parameter v, the item's decision signal D_i , and zero-centered normally distributed noise with standard deviation σ:

$$E_i(t) = E_i(t-1) + v \times D_i + N(0, \sigma^2) \text{ with } E_i(t < t0_i) = 0 \quad (9)$$

As for the PSM, we re-scaled all liking ratings to a range from 1 to 7 to ensure $D_i > 0$. Note that we set $E_i(t < t0_i) = 0$ for all items that were not yet looked at by time point t.

Lastly, the first passage time density $f_i(t)$ of a single linear stochastic accumulator $E_i(t)$ at time point *t* is given by the Inverse Gaussian Distribution (Wald, 2004):

$$f_i(t) = \left[\frac{\lambda}{2 \times \pi \times t^3}\right]^{1/2} \times exp\left\{\frac{-\lambda \times (t-\mu)^2}{2 \times \mu^2 \times t}\right\} \text{ with } \mu = \frac{b}{v \times D_i} \text{ and } \lambda = \frac{b^2}{\sigma^2}. \quad (10)$$

With a cumulative distribution function $F_i(t)$ of:

$$F_i(t) = \Phi \times \left(\sqrt{\frac{\lambda}{t}} \times \left(\frac{t}{\mu} - 1\right)\right) + exp\left(\frac{2 \times \lambda}{\mu}\right) \times \Phi \times \left(-\sqrt{\frac{\lambda}{t}} \times \left(\frac{t}{\mu} + 1\right)\right), \quad (11)$$

where Φ is the standard normal cumulative distribution function.

Yet, $f_i(t)$ does not take into account that there are multiple accumulators in each trial racing towards the same decision boundary. A choice is made as soon as any of these accumulators reaches the boundary. Therefore, we correct $f_i(t)$ for the probability that any other accumulator *i* crosses the boundary first, to obtain the joint probability $p_i(t)$ of an accumulator reaching the boundary at the empirically observed response time *RT*, and no other accumulator *j* having reached it prior to *RT*:

$$p_i(RT) = f_i(RT - t0_i) \times \prod_{j \epsilon J} \left(1 - F_j\left(RT - t0_j\right)\right) \quad (12)$$

Gaze-weighted linear accumulator model (GLAM)

The GLAM (Thomas et al., 2019; Molter et al., 2019) assumes that choices are driven by the accumulation of noisy evidence in favor of each available choice alternative *i*. As for the IAM, a choice is determined by the first accumulator that reaches a common pre-defined decision boundary *b* ($b = 1$). Particularly, the accumulated evidence E_i in favor of alternative *i* is defined as a stochastic process that changes at each point in time *t* ($\Delta t = 1ms$) according to:

$$E_i(t) = E_i(t-1) + v \times D_i + N(0, \sigma^2) \text{ with } E_i(0) = 0 \quad (13)$$

E_i consists of a drift term D_i and zero-centered normally distributed noise with standard deviation σ. Note that we only included choice alternatives in the decision process that were also looked at in a trial (by setting $E_i(t) = 0$ for all other alternatives). The overall speed of the accumulation process is determined by the velocity parameter v. The drift term D_i is a function of a set of decision signals for each item *i*: an absolute and a relative decision signal. The absolute decision signal implements the model's gaze bias mechanism. Importantly, the variant of the GLAM used here extends the gaze bias mechanism of the original GLAM upon an additive influence of gaze on the decision process (in line with recent empirical findings; Cavanagh, Wiecki, Kochar & Frank, 2014; Westbrook et al., 2020). The absolute decision signal can thereby be in two states: An additive state, in which the item's value l_i (as indicated by the item's liking rating) is amplified by a positive constant ζ $(0 \leq \zeta \leq 10)$ while the item is looked at, and a multiplicative state while any other item is looked at, where the item value l_i is discounted by γ ($0 \leq \gamma \leq 1$). The average absolute decision signal A_i is then given by

$$A_i = g_i \times (l_i + \zeta) + (1 - g_i) \times \gamma \times l_i \tag{14}$$

Here, g_i describes the fraction of total trial time that the decision maker spends looking at item *i.* To obtain the passive-gaze variant of the GLAM, we set $\gamma = 1$and $\zeta = 0$.

We define the relative decision signal R_i as the difference in the average absolute decision signal A_i of item *i* and the maximum of all other absolute decision signals *J*:

$$R_i = A_i - max_{j \epsilon J}(A_j) \tag{15}$$

The GLAM further assumes that the decision process is particularly sensitive to small differences in the relative decision signals R_i which are close to 0 (where the average absolute decision signal A_i for an item *i* is close to the maximum of all other items *J*). To account for this, the GLAM scales the relative decision signals R_i by the use of a logistic transform $\sigma$with scaling parameter τ:

$$D_i = \sigma(R_i) \tag{16}$$

$$\sigma(x) = \frac{1}{1 + exp(-\tau \times x)} \tag{17}$$

This transform also ensures that the drift terms D_i of the stochastic race are positive, whereas the relative decision signals R_i can be positive and negative (eq. 15).

Similar to the independent evidence accumulation model (see eqs. 10-12), we can obtain the joint probability $p_i(t)$ of an accumulator reaching the boundary at time *t*, and no other accumulator *j* having reached it prior to *t,* as follows:

$$p_i(t) = f_i(t) \times \prod_{j \epsilon J}\left(1 - F_j(t)\right) \tag{18}$$

Note that *f(t)* and *F(t)* follow eq. 10-11.

Parameter estimation

All model parameters were estimated separately for each individual in each set size condition. The individual models were implemented in the Python library PyMC3.9.1 (Salvatier, Wiecki & Fonnesbeck, 2016) and fitted using Markov Chain Monte Carlo Metropolis sampling. For each model, we first sampled 5000 tuning samples that were then discarded (burn-in), before drawing another 5000 additional posterior samples that we used to estimate the model parameters. Each parameter trace was checked for convergence by means of the Gelman–Rubin statistic ($|\hat{R} - 1| < 0.05$) as well as the mean number of effective samples (> 100). If a trace did not converge, we re-sampled the model and increased the number of burn-in samples by 5000 until convergence was achieved. Note that the IAM+ did not converge for three, one, one, and one subjects in the choice set sizes with 9, 16, 25, and 36 items respectively after 50 re-sampling attempts. Similarly, the IAM did not converge for one subject in the choice set size with 25 items. For these subjects, we continued all analyses with the model that was sampled last. We defined all model parameter estimates as maximum a posteriori estimates (MAP) of the resulting posterior traces (for an overview, see Figure 5-figure supplement 1 and Supplementary Files 5-7).

Probabilistic satisficing model

The probabilistic satisficing model has five parameters, which determine the additive (ζ) and multiplicative (γ) gaze bias effects on its cached value, the influence of cached value (α) and time (υ) on its stopping probability, and the sensitivity of its softmax choice rule (τ). We placed uninformative, uniform priors on all model parameters:

- ζ ~ Uniform(0, 10)
- γ ~ Uniform(0, 1)
- υ ~ Uniform(0, 0.001)
- α ~ Uniform(0, 0.001)
- τ ~ Uniform(0, 10)

Independent evidence accumulation model

The independent evidence accumulation model has four parameters, which determine its general accumulation speed (υ) and noise (σ) and its additive (ζ) and multiplicative (γ) gaze bias effects. We placed uninformative, uniform priors on all model parameters:

- υ ~ Uniform(1e-7, 0.005)
- σ ~ Uniform(1e-7, 0.05)
- ζ ~ Uniform(0, 10)
- γ ~ Uniform(0, 1)

Gaze-weighted linear accumulator model

The GLAM variant used here has five parameters, which determine its general accumulation speed (υ) and noise (σ), its additive (ζ) and multiplicative (γ) gaze bias, and the sensitivity of the scaling of the relative decision signals (τ). We placed uninformative, uniform priors between on all model parameters:

- υ ~ Uniform(1e-7, 0.005)
- σ ~ Uniform(1e-7, 0.05)
- ζ ~ Uniform(0, 10)

- γ ~ Uniform(0, 1)
- τ ~ Uniform(0, 10)

Error likelihood model

In line with existing DDM toolboxes (e.g., Wiecki, Sofer & Frank, 2013), we include spurious trials at a fixed rate of 5% in all model estimation procedures (see eq. 20). We model these spurious trials with a subject-specific uniform likelihood distribution u_s. This likelihood describes the probability of a random choice for any of the N available items at a random time point in the range of a subject's empirically observed response times rt_s (Ratcliff & Tuerlinckx, 2002):

$$u_s(t) = \frac{1}{N \times (max(rt_s) - min(rt_s))} \tag{19}$$

The resulting likelihood $l_{s,i}(t)$ of subject s choosing item i at time t for all estimated models was thereby given by:

$$l_{s,i}(t) = 0.95 \times p_i(t) + 0.05 \times u_s(t) \tag{20}$$

Model simulations

We repeated the data of each trial 50 times during the simulation and simulated a choice and RT for each trial with each model at a rate of 95%, while we simulated random choices and RTs according to eq. 19 at a rate of 5%. We defined the model parameter estimates that were used for the simulation as the maximum a posteriori estimates (MAP) of the posterior traces of the individual subject models (see Figure 5-figure supplement 1 and Supplementary Files 5-7).

Probabilistic satisficing model

For each trial repetition, we simulated a choice and response time according to eqs. 1 and 6.

Independent evidence accumulation model

For each trial repetition, we simulated a choice and RT by first drawing a first passage time (FPT_i) for each item i in a choice set according to eq. 10. To account for the gaze-dependent onsets of evidence accumulation, we then added the empirically observed time at which the item was first looked at in a trial ($t0_i$, see eqs. 9, 12) to the drawn FPT_i of each item. The item with the shortest $FPT_i + t0_i$ then determined the RT and choice.

GLAM

For each trial repetition, we simulated a choice and response time by first drawing a first passage time (FPT_i) for each item in a choice set according to eq. 10. The item with the shortest FPT_i then determined the RT and choice.

Mixed-effects modelling

All mixed effects models were fitted in a Bayesian hierarchical framework by the use of the Bayesian Model-Building Interface (bambi 0.2.0; Yarkoni & Westfall, 2016). Bambi automatically generates weakly informative priors for all model variables. We fitted all models using the Markov Chain Monte Carlo No-U-Turn-Sampler (NUTS; Hoffman & Gelman, 2014), by drawing 2000 samples from the posterior, after a minimum of 500 burn-in samples. In addition to the reported fixed effect estimates, all models included random intercepts for each subject, as well as random subject-slopes for each model coefficient. The posterior traces of all reported fixed effects estimates were checked for convergence by means of the Gelman–Rubin statistic ($|\hat{R} - 1| < 0.05$). If a fixed effect posterior trace did not converge, the model was re-sampled and the number of burn-in samples increased by 2000 until convergence was achieved.

Software

All data analyses were performed in Python 3.6.8 (Python Software Foundation), by the use of the SciPy 1.3.1, (Virtanen et al., 2019), NumPy 1.17.3 (Oliphant, 2006), Matplotlib 3.1.1 (Hunter, 2017), Pandas 0.25.2 (McKinney, 2010), Theano 1.0.4 (Theano Development Team, 2016), bambi 0.2.0 (Yarkoni & Westfall, 2016), ArviZ 0.9.0 (Kumar, Carroll, Hartikainen & Martin, 2019), and PyMC3.9.1 (Salvatier, Wiecki, & Fonnesbeck, 2016) packages. For the computation of stimulus metrics, we further utilized the Pillow 5.0 (http://pillow.readthedocs.io) Python package. The experiment was written in MATLAB (The MathWorks, Inc., Natick, Massachusetts, United States), using the Psychophysics Toolbox extensions (Brainard, 1997).

Availability of data, model and analysis code

All experiment stimuli, data and analysis scripts are available at: github.com/athms/many-item-choice

Acknowledgments

Armin W. Thomas is funded by the Max Planck Institute for Human Development. Felix Molter is supported by the International Max Planck Research School on the Life Course (LIFE). Ian Krajbich is funded by National Science Foundation Career Award 1554837 and the Cattell Sabbatical Fund. All data were collected in the Rangel Neuroeconomics Laboratory. Antonio Rangel was also involved in conceiving the experiment. Thanks to Wenjia Zhao for comments on the manuscript.

Competing interest statement

The authors declare no competing interests.

Supplementary files

1. Supplementary Files 1-4: Exemplar visual search trajectories for choice sets with 9 (File 1), 16 (File 2), 25 (File 3), and 36 (File 4) alternatives. Each video shows the visual search trajectory over the choice screen for one exemplary trial of each choice set size condition. The current gaze position is indicated by a white box, while the choice is indicated by a red box. For better visibility, gaze durations have been increased by a factor of two.
2. Supplementary File 5: Mean parameter estimates of the probabilistic satisficing model with active (PSM+) and passive (PSM) account of gaze in the decision process for each choice set size. The probabilistic satisficing model has five parameters, determining the additive (ζ) and multiplicative (γ) gaze bias effects on its cached value, the influence of cached value (α) and time (v) on its stopping probability, and the sensitivity of its softmax choice rule (τ). Note that the high mean value of α for the active-gaze variant in the choice set size with 16 items is driven by one outlier (see Figure 5-figure supplement 1 D).
3. Supplementary File 6: Mean parameter estimates of the independent evidence accumulation model with active (IAM+) and passive (IAM) account of gaze in the decision process for each choice set size. The independent evidence accumulation model has four parameters, determining its additive (ζ) and multiplicative (γ) gaze bias effects and its general accumulation speed (v) and noise (σ).
4. Supplementary File 7: Mean parameter estimates for the gaze-weighted linear accumulator model with active (GLAM+) and passive (GLAM) account of gaze in the decision process for each choice set size. The GLAM variant used in this work has five parameters, determining its additive (ζ) and multiplicative (γ) gaze bias, its general accumulation speed (v) and noise (σ) as well as the sensitivity of the scaling of the relative decision signals (τ).

References

Alós-Ferrer, C. (2018). A Dual-Process Diffusion Model. Journal of Behavioral Decision Making, 31(2), 203-218. doi.org/10.1002/bdm.1960

Amasino, D. R., Sullivan, N. J., Kranton, R. E., & Huettel, S. A. (2019). Amount and time exert independent influences on intertemporal choice. Nature human behaviour, 3(4), 383-392. doi.org/10.1038/s41562-019-0537-2

Armel, K. C., Beaumel, A., & Rangel, A. (2008). Biasing simple choices by manipulating relative visual attention. Judgment and Decision Making, 3(5), 396.

Ashby, N. J., Jekel, M., Dickert, S., & Glöckner, A. (2016). Finding the right fit: A comparison of process assumptions underlying popular drift-diffusion models. Journal of Experimental Psychology: Learning, Memory, and Cognition, 42(12), 1982. doi.org/10.1037/xlm0000279

Berkowitsch, N. A., Scheibehenne, B., & Rieskamp, J. (2014). Rigorously testing multialternative decision field theory against random utility models. Journal of Experimental Psychology: General, 143(3), 1331. doi.org/10.1037/a0035159

Bhatia, S. (2013). Associations and the accumulation of preference. Psychological review, 120(3), 522. doi.org/10.1037/a0032457

Boorman, E. D., Rushworth, M. F., & Behrens, T. E. (2013). Ventromedial prefrontal and anterior cingulate cortex adopt choice and default reference frames during sequential multi-alternative choice. Journal of Neuroscience, 33(6), 2242-2253. doi.org/10.1523/JNEUROSCI.3022-12.2013

Brainard, D. H. (1997). The psychophysics toolbox. Spatial Vision, 10(4), 433-436. doi.org/10.1163/156856897X00357

Brown, S. D., & Heathcote, A. (2008). The simplest complete model of choice response time: Linear ballistic accumulation. Cognitive Psychology, 57(3), 153-178. doi.org/10.1016/j.cogpsych.2007.12.002

Caplin, A., Dean, M., & Leahy, J. (2019). Rational inattention, optimal consideration sets, and stochastic choice. The Review of Economic Studies, 86(3), 1061-1094. doi.org/10.1093/restud/rdy037

Caplin, A., Dean, M., & Martin, D. (2011). Search and satisficing. American Economic Review, 101(7), 2899-2922. doi.org/10.1257/aer.101.7.2899

Cavanagh, S. E., Malalasekera, W. N., Miranda, B., Hunt, L. T., & Kennerley, S. W. (2019). Visual fixation patterns during economic choice reflect covert valuation processes that emerge with learning. Proceedings of the National Academy of Sciences, 116(45), 22795-22801. doi.org/doi.org/10.1073/pnas.1906662116

Cavanagh, J. F., Wiecki, T. V., Kochar, A., & Frank, M. J. (2014). Eye tracking and pupillometry are indicators of dissociable latent decision processes. Journal of Experimental Psychology: General, 143(4), 1476. doi.org/10.1037/a0035813

Chandon, P., Hutchinson, J. W., Bradlow, E. T., & Young, S. H. (2009). Does in-store marketing work? Effects of the number and position of shelf facings on brand attention and evaluation at the point of purchase. Journal of Marketing, 73(6), 1-17. doi.org/10.1509/jmkg.73.6.1

Chow, Y. S. & Robbins, Herbert. (1961). A Martingale System Theorem and Applications. Proceedings of the Fourth Berkeley Symposium on Mathematical Statistics and Probability, Volume 1: Contributions to the Theory of Statistics, 93--104, University of California Press, Berkeley

Churchland, A. K., Kiani, R., & Shadlen, M. N. (2008). Decision-making with multiple alternatives. Nature Neuroscience, 11(6), 693. doi.org/10.1038/nn.2123

Clithero, J. A. (2018). Improving out-of-sample predictions using response times and a model of the decision process. Journal of Economic Behavior & Organization, 148, 344-375. doi.org/10.1016/j.jebo.2018.02.007

De Martino, B., Kumaran, D., Seymour, B., & Dolan, R. J. (2006). Frames, biases, and rational decision-making in the human brain. Science, 313(5787), 684-687. doi.org/10.1126/science.1128356

Diederich, A. (2003). MDFT account of decision making under time pressure. Psychonomic Bulletin & Review, 10(1), 157-166. doi.org/10.3758/BF03196480

Fellner, G., Güth, W., & Maciejovsky, B. (2009). Satisficing in financial decision making - a theoretical and experimental approach to bounded rationality. Journal of Mathematical Psychology, 53(1), 26-33. doi.org/10.1016/j.jmp.2008.11.004

Fellows, L. K. (2006). Deciding how to decide: ventromedial frontal lobe damage affects information acquisition in multi-attribute decision making. Brain, 129(4), 944-952. doi.org/10.1093/brain/awl017

Fisher, G. (2017). An attentional drift diffusion model over binary-attribute choice. Cognition, 168, 34-45. doi.org/10.1016/j.cognition.2017.06.007

Folke, T., Jacobsen, C., Fleming, S. M., & De Martino, B. (2017). Explicit representation of confidence informs future value-based decisions. Nature Human Behaviour, 1(1), 0002. doi.org/10.1038/s41562-016-0002

Gigerenzer, G., & Goldstein, D. G. (1996). Reasoning the fast and frugal way: models of bounded rationality. Psychological review, 103(4), 650. doi.org/10.1037/0033-295X.103.4.650

Gluth, S., Spektor, M. S., & Rieskamp, J. (2018). Value-based attentional capture affects multi-alternative decision making. Elife, 7, e39659. doi.org/10.7554/eLife.39659

Gluth, S., Kern, N., Kortmann, M., & Vitali, C. L. (2020). Value-based attention but not divisive normalization influences decisions with multiple alternatives. Nature Human Behaviour, 1-12. doi.org/10.1038/s41562-020-0822-0

Hare, T. A., Camerer, C. F., & Rangel, A. (2009). Self-control in decision-making involves modulation of the vmPFC valuation system. Science, 324(5927), 646-648. doi.org/10.1126/science.1168450

Hauser, J. R., & Wernerfelt, B. (1990). An evaluation cost model of consideration sets. Journal of consumer research, 16(4), 393-408.

Hunt, L. T., Malalasekera, W. N., de Berker, A. O., Miranda, B., Farmer, S. F., Behrens, T. E., & Kennerley, S. W. (2018). Triple dissociation of attention and decision computations across prefrontal cortex. Nature Neuroscience, 21(10), 1471-1481. doi.org/10.1038/s41593-018-0239-5

Hunter, J. D. (2007). Matplotlib: A 2D graphics environment. Computing in science & engineering, 9(3), 90-95. doi.org/10.1109/MCSE.2007.55

Hutcherson, C. A., Bushong, B., & Rangel, A. (2015). A neurocomputational model of altruistic choice and its implications. Neuron, 87(2), 451-462. doi.org/10.1016/j.neuron.2015.06.031

Konovalov, A., & Krajbich, I. (2016). Gaze data reveal distinct choice processes underlying model-based and model-free reinforcement learning. Nature Communications, 7, 12438. doi.org/10.1038/ncomms12438

Krajbich, I., Armel, C., & Rangel, A. (2010). Visual fixations and the computation and comparison of value in simple choice. Nature Neuroscience, 13(10), 1292. doi.org/10.1038/nn.2635

Krajbich, I., & Rangel, A. (2011). Multialternative drift-diffusion model predicts the relationship between visual fixations and choice in value-based decisions. Proceedings of the National Academy of Sciences, 108(33), 13852-13857. doi.org/10.1073/pnas.1101328108

Krosnick, J. A. (1991). Response strategies for coping with the cognitive demands of attitude measures in surveys. Applied cognitive psychology, 5(3), 213-236. doi.org/10.1002/acp.2350050305

Kumar, R., Carroll, C., Hartikainen, A., & Martín, O. A. (2019). ArviZ a unified library for exploratory analysis of Bayesian models in Python.

Luce, R. D., & Raiffa, H. (1957). Games and decisions. New York, John Wiley Sons.

Masatlioglu, Y., Nakajima, D., & Ozbay, E. Y. (2012). Revealed attention. American Economic Review, 102(5), 2183-2205. doi.org/10.1257/aer.102.5.2183

Matějka, F., & McKay, A. (2015). Rational inattention to discrete choices: A new foundation for the multinomial logit model. American Economic Review, 105(1), 272-98. doi.org/10.1257/aer.20130047

McCall, J. J. (1970). Economics of information and job search. The Quarterly Journal of Economics, 113-126. doi.org/10.2307/1879403

McGinty, V. B., Rangel, A., & Newsome, W. T. (2016). Orbitofrontal cortex value signals depend on fixation location during free viewing. Neuron, 90(6), 1299-1311. doi.org/10.1016/j.neuron.2016.04.045

McKinney, W. (2010, June). Data structures for statistical computing in python. In Proceedings of the 9th Python in Science Conference (Vol. 445, pp. 51-56). doi.org/10.25080/Majora-92bf1922-00a

Molter, F., Thomas, A. W., Heekeren, H. R., & Mohr, P. N. C. (2019). GLAMbox: A Python toolbox for investigating the association between gaze allocation and decision behaviour. PLoS ONE, *14*(12). doi.org/10.1371/journal.pone.0226428

Mormann, M. M., Malmaud, J., Huth, A., Koch, C., & Rangel, A. (2010). The drift diffusion model can account for the accuracy and reaction time of value-based choices under high and low time pressure. Judgement and Decision Making, 5(6), 437-449. doi.org/10.2139/ssrn.1901533

Noguchi, T., & Stewart, N. (2014). In the attraction, compromise, and similarity effects, alternatives are repeatedly compared in pairs on single dimensions. Cognition, 132(1), 44-56. doi.org/10.1016/j.cognition.2014.03.006

Oliphant, T. E. (2006). A guide to NumPy (Vol. 1, p. 85). USA: Trelgol Publishing.

Payne, J. W. (1976). Task complexity and contingent processing in decision making: An information search and protocol analysis. Organizational behavior and human performance, 16(2), 366-387. doi.org/10.1016/0030-5073(76)90022-2

Philiastides, M. G., & Ratcliff, R. (2013). Influence of branding on preference-based decision making. Psychological Science, 24(7), 1208-1215. doi.org/10.1177/0956797612470701

Pieters, R., & Warlop, L. (1999). Visual attention during brand choice: The impact of time pressure and task motivation. International Journal of research in Marketing, 16(1), 1-16. doi.org/10.1016/S0167-8116(98)00022-6

Polania, R., Woodford, M., & Ruff, C. C. (2019). Efficient coding of subjective value. Nature Neuroscience, 22(1), 134-142. doi.org/10.1038/s41593-018-0292-0

Pärnamets, P., Johansson, P., Hall, L., Balkenius, C., Spivey, M. J., & Richardson, D. C. (2015). Biasing moral decisions by exploiting the dynamics of eye gaze. Proceedings of the National Academy of Sciences, 112(13), 4170-4175. doi.org/10.1073/pnas.1415250112

Rapoport, A., & Tversky, A. (1966). Cost and accessibility of offers as determinants of optional stopping. Psychonomic Science, 4(1), 145-146. doi.org/10.3758/BF03342220

Ratcliff, R., & Tuerlinckx, F. (2002). Estimating parameters of the diffusion model: Approaches to dealing with contaminant reaction times and parameter variability. Psychonomic Bulletin & Review, 9(3), 438-481. doi.org/10.3758/BF03196302

Reutskaja, E., Nagel, R., Camerer, C. F., & Rangel, A. (2011). Search dynamics in consumer choice under time pressure: An eye-tracking study. American Economic Review, 101(2), 900-926. doi.org/10.1257/aer.101.2.900

Robbins, H., Sigmund, D., & Chow, Y. (1971). Great expectations: the theory of optimal stopping. Houghton-Nifflin, 7, 631-640.

Roberts, J. H., & Lattin, J. M. (1991). Development and testing of a model of consideration set composition. Journal of Marketing Research, 28(4), 429-440. doi.org/10.2307/3172783

Rodriguez, C. A., Turner, B. M., & McClure, S. M. (2014). Intertemporal choice as discounted value accumulation. PloS one, 9(2). doi.org/10.1371/journal.pone.0090138

Roe, R. M., Busemeyer, J. R., & Townsend, J. T. (2001). Multialternative decision field theory: A dynamic connectionst model of decision making. Psychological review, 108(2), 370. doi.org/10.1037//0033-295X.108.2.370

Russo, J. E., & Rosen, L. D. (1975). An eye fixation analysis of multialternative choice. Memory & Cognition, 3(3), 267-276. doi.org/10.3758/BF03212910

Salvatier J, Wiecki T. V., Fonnesbeck C. (2016) Probabilistic programming in Python using PyMC3.

PeerJ Computer Science 2:e55. doi.org/10.7717/peerj-cs.55

Schwartz, B., Ward, A., Monterosso, J., Lyubomirsky, S., White, K., & Lehman, D. R. (2002). Maximizing versus satisficing: Happiness is a matter of choice. Journal of Personality and Social Psychology, 83(5), 1178. doi.org/10.1037/0022-3514.83.5.1178

Virtanen, P., Gommers, R., Oliphant, T. E., Haberland, M., Reddy, T. et al. (2019). SciPy 1.0--fundamental algorithms for scientific computing in Python. arXiv preprint arXiv:1907.10121.

Shimojo, S., Simion, C., Shimojo, E., & Scheier, C. (2003). Gaze bias both reflects and influences preference. Nature Neuroscience, 6(12), 1317. doi.org/10.1038/nn1150

Simon, H. A. (1955). A behavioral model of rational choice. The Quarterly Journal of Economics, 69(1), 99-118. doi.org/10.2307/1884852

Simon, H. A. (1956). Rational choice and the structure of the environment. Psychological review, 63(2), 129. doi.org/10.1037/h0042769

Simon, H. A. (1957). Models of man; social and rational. doi.org/10.1177/001316446102100129

Simon, H. A. (1959). Theories of decision-making in economics and behavioral science. The American Economic Review, 49(3), 253-283. doi.org/10.1007/978-1-349-00210-8_1

Sims, C. A. (2003). Implications of rational inattention. Journal of monetary Economics, 50(3), 665-690. doi.org/10.1016/S0304-3932(03)00029-1

Smith, S. M., & Krajbich, I. (2019). Gaze amplifies value in decision making. Psychological Science, 30(1), 116-128. doi.org/10.1177/0956797618810521

Smith, P. L., & Vickers, D. (1988). The accumulator model of two-choice discrimination. Journal of Mathematical Psychology, *32*(2), 135-168. doi.org/10.1016/0022-2496(88)90043-0

Stewart, N., Hermens, F., & Matthews, W. J. (2016). Eye movements in risky choice. Journal of Behavioral Decision Making, 29(2-3), 116-136. doi.org/10.1002/bdm.1854

Stüttgen, P., Boatwright, P., & Monroe, R. T. (2012). A satisficing choice model. Marketing Science, 31(6), 878-899. doi.org/10.1287/mksc.1120.0732

The Theano Development Team (2016). Theano: A Python framework for fast computation of mathematical expressions. arXiv preprint arXiv:1605.02688.

Thomas, A. W., Molter, F., Krajbich, I., Heekeren, H. R., & Mohr, P. N. (2019). Gaze bias differences capture individual choice behaviour. Nature Human Behaviour, 3(6), 625. doi.org/10.1038/s41562-019-0584-8

Towal, R. B., Mormann, M., & Koch, C. (2013). Simultaneous modeling of visual saliency and value computation improves predictions of economic choice. Proceedings of the National Academy of Sciences, 110(40), E3858-E3867. doi.org/10.1073/pnas.1304429110

Trueblood, J. S., Brown, S. D., & Heathcote, A. (2014). The multiattribute linear ballistic accumulator model of context effects in multialternative choice. Psychological Review, 121(2), 179. doi.org/10.1037/a0036137

Usher, M., Olami, Z., & McClelland, J. L. (2002). Hick's law in a stochastic race model with speed–accuracy tradeoff. Journal of Mathematical Psychology, 46(6), 704-715. doi.org/10.1006/jmps.2002.1420

Usher, M., & McClelland, J. L. (2004). Loss aversion and inhibition in dynamical models of multialternative choice. Psychological Review, 111(3), 757. doi.org/10.1037/0033-295X.111.3.757

Vaidya, A. R., & Fellows, L. K. (2015). Testing necessary regional frontal contributions to value assessment and fixation-based updating. Nature Communications, 6, 10120. doi.org/10.1038/ncomms10120

Vehtari, A., Gelman, A., & Gabry, J. (2017). Practical Bayesian model evaluation using leave-one-out cross-validation and WAIC. Statistics and Computing, 27(5), 1413-1432. doi.org/10.1007/s11222-016-9696-4

Wald, A. (2004). Sequential analysis. Courier Corporation.

Webb, R. (2019). The (neural) dynamics of stochastic choice. Management Science, *65*(1), 230-255. doi.org/10.1287/mnsc.2017.2931

Westbrook, A., van den Bosch, R., Määttä, J. I., Hofmans, L., Papadopetraki, D., Cools, R., & Frank, M. J. (2020). Dopamine promotes cognitive effort by biasing the benefits versus costs of cognitive work. Science, *367*(6484), 1362-1366. doi.org/10.1126/science.aaz5891

Wiecki, T. V., Sofer, I., & Frank, M. J. (2013). HDDM: hierarchical bayesian estimation of the drift-diffusion model in python. Frontiers in Neuroinformatics, 7, 14. doi.org/10.3389/fninf.2013.00014

Yarkoni, T., & Westfall, J. (2016, September 18). Bambi: A simple interface for fitting Bayesian mixed effects models. doi.org/10.31219/osf.io/rv7sn

Figure supplements

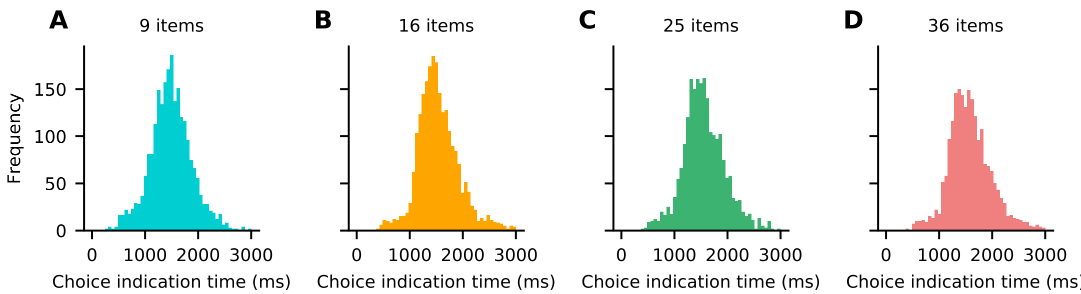

Figure 1-figure supplement 1. Choice indication times for each choice set size as indicated by the time difference between space bar press (indicating RT) and subsequent mouse click on a snack food item image. For details on the experiment paradigm, see the "Methods" section of the main text. Choice indication times generally increased with the Euclidean distance of the chosen item from the screen center (where the mouse cursor appeared) as well as choice set size (intercept = 1256 ms, 94% HDI = [1178, 1337], β = 0.59 ms, 94% HDI = [0.52, 0.66] per pixel increase in Euclidean distance, 2.3 ms, 94% HDI = [1.6, 3] per item). Note that the intercept estimate of 1256 ms describes the average time that it took subjects to move their hand from the space bar to the computer mouse and added time resulting from movement noise in the mouse trajectory.

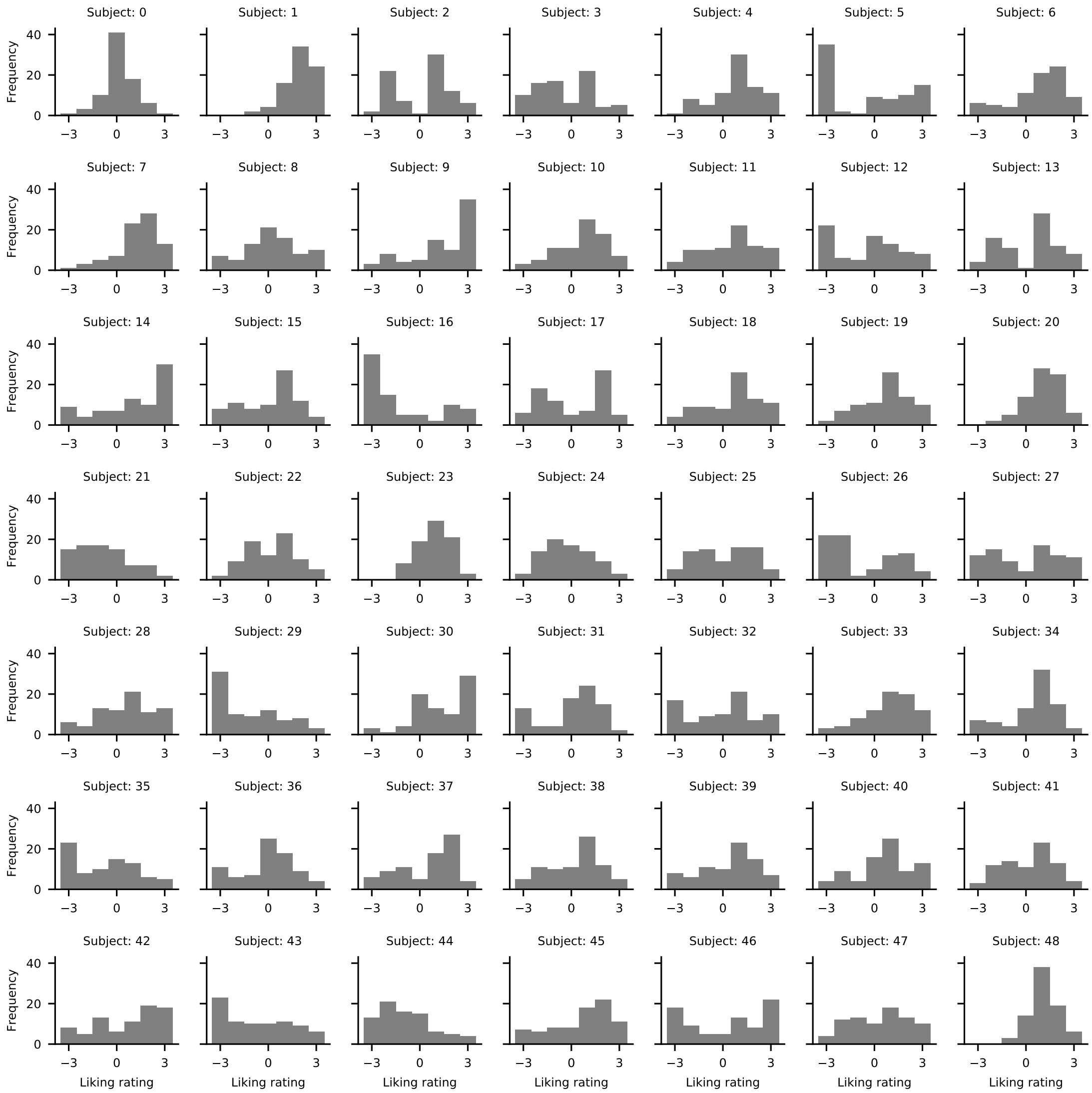

Figure 1-figure supplement 2. Liking rating distribution of each subject.

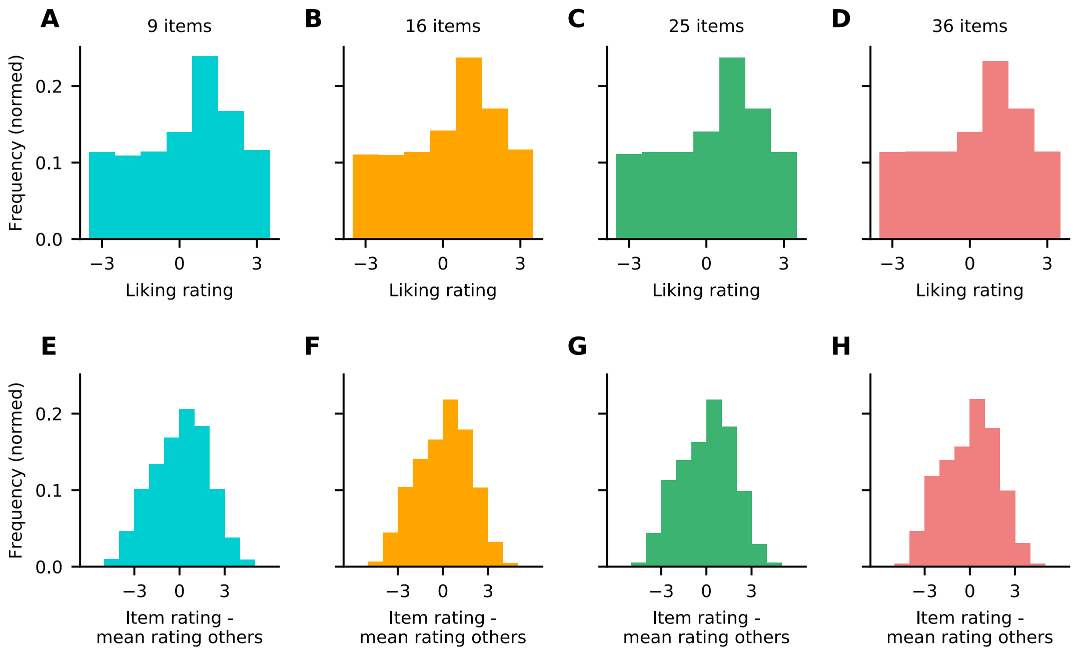

Figure 1-figure supplement 3. Absolute (A-D) and relative (E-H; defined as the difference between an item's rating and the mean rating of the other items in a choice set) liking rating distributions for each choice set size.

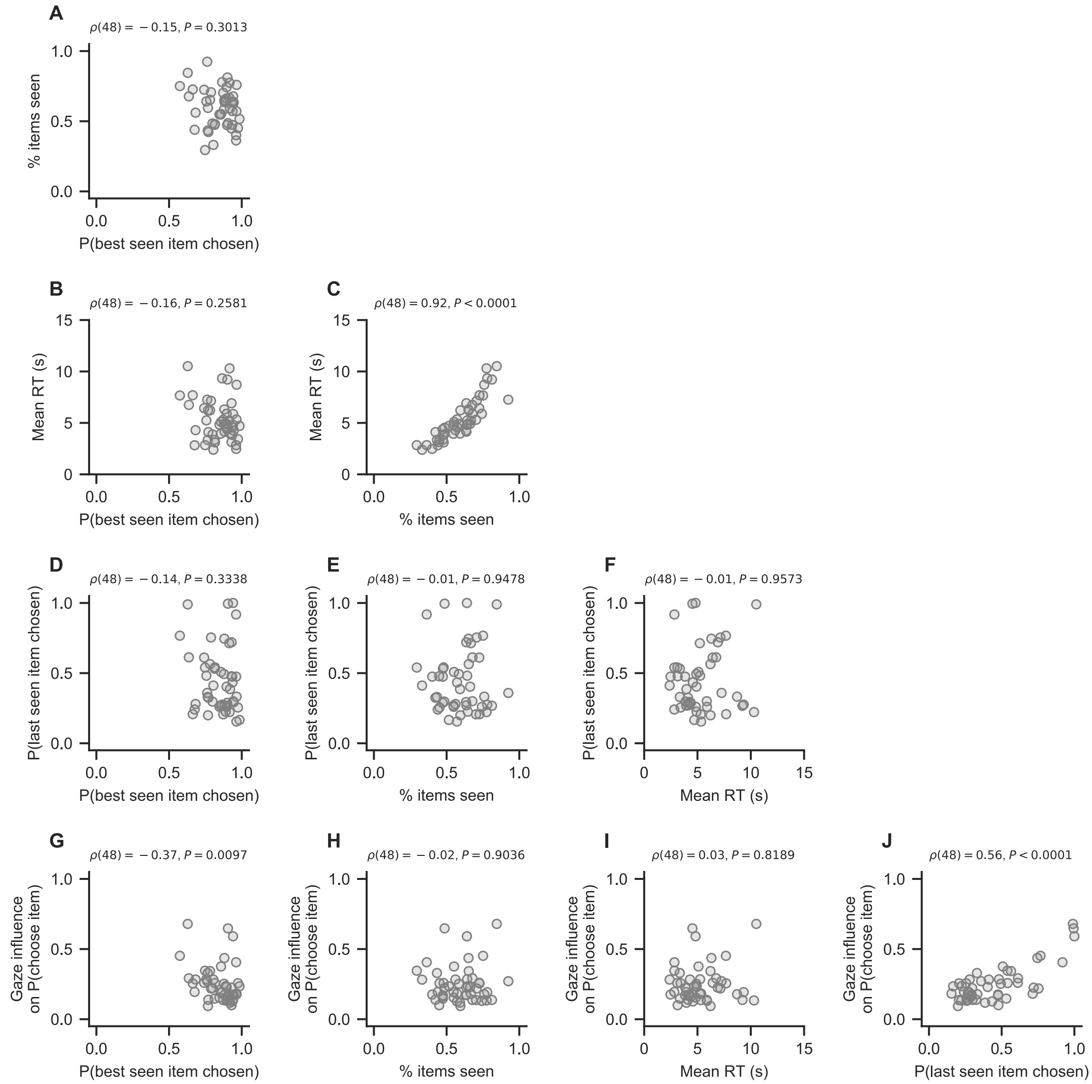

Figure 4-figure supplement 1. Detailed view of the associations of the choice psychometrics presented in Fig. 4 F of the main text. Scatter points indicate pooled subject means across the choice set sizes. Due to non-normal distributions of the pooled subject means Spearman's rank correlation coefficients (ρ) with corresponding P-values are reported for each association.

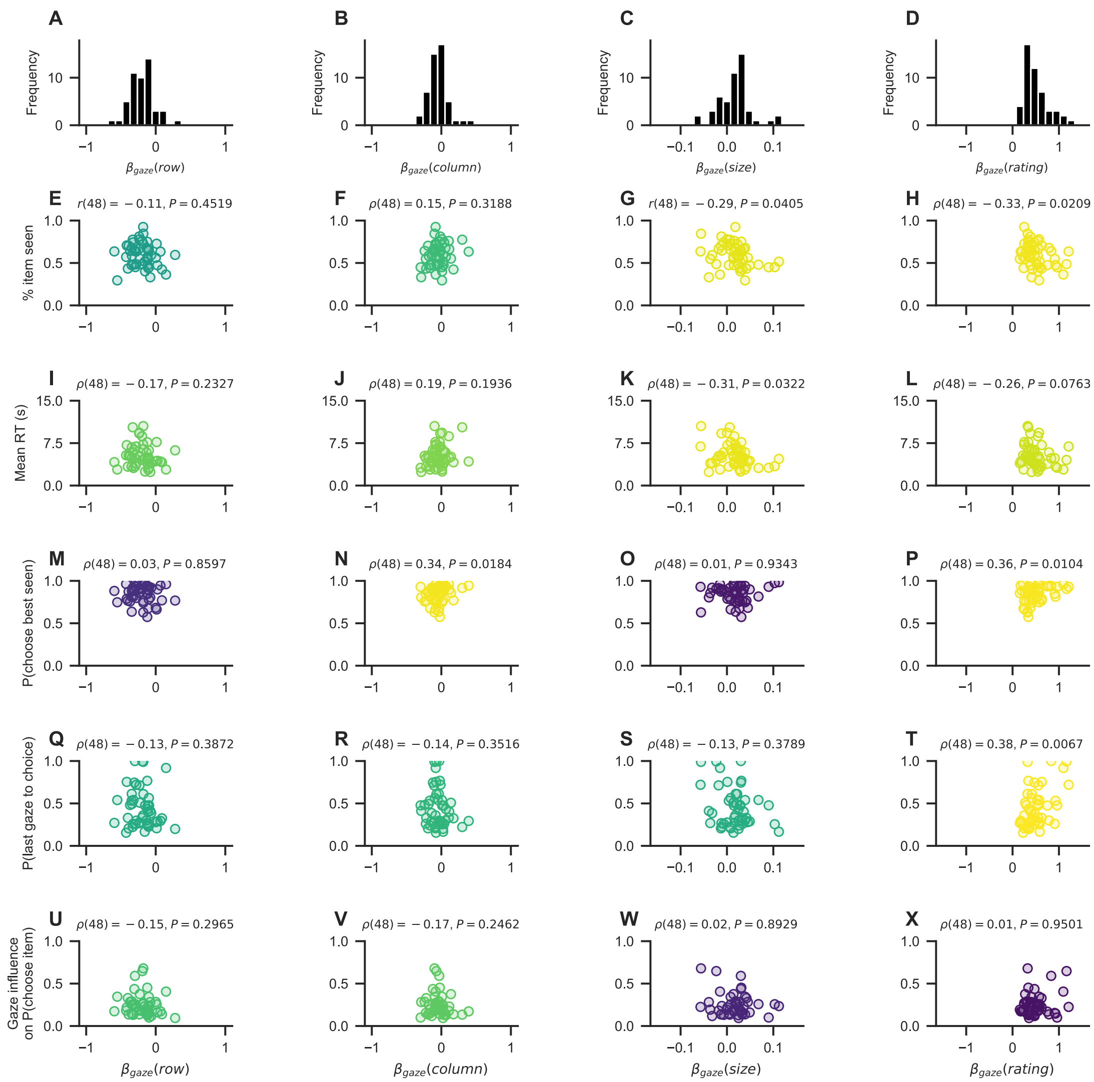

Figure 4-figure supplement 2. Association between the choice psychometrics presented in Fig. 4 A-E of the main text and a set of measures describing individuals' visual search behaviour. To quantify individuals' visual search, we computed a mixed effects regression model for each individual in the data, estimating how much the individual's allocation of cumulative gaze to an item (measured as the fraction of trial time that the item was looked at) is influenced by the item's attributes (namely, the item's row- and column-position, size, and liking rating; for details on the item attributes, see the "Methods" section of the main text) as well as the choice set size, resulting in one coefficient estimate (β_{gaze}) for the influence of each item attribute and choice set size on the distribution of cumulative gaze. We then

studied the relationship between the resulting regression estimate (β_{gaze} ; A-D) for each of the item attributes and each individuals' pooled mean on the five behavioral choice metrics presented in Fig. 4 A-E of the main text (namely, the mean fraction of items looked at in a trial, mean RT, the probability of choosing the highest-rated seen item from a choice set, the probability of looking at the chosen item last, and the gaze influence measure). Pearson's r correlation coefficient with P-value is indicated for each association. If the assumption of normality is violated, Spearman's rank correlation coefficient (ρ) with P-value is reported instead. Brighter yellow colors indicate smaller P-values. Scatter points indicate pooled subject means across the choice set sizes.

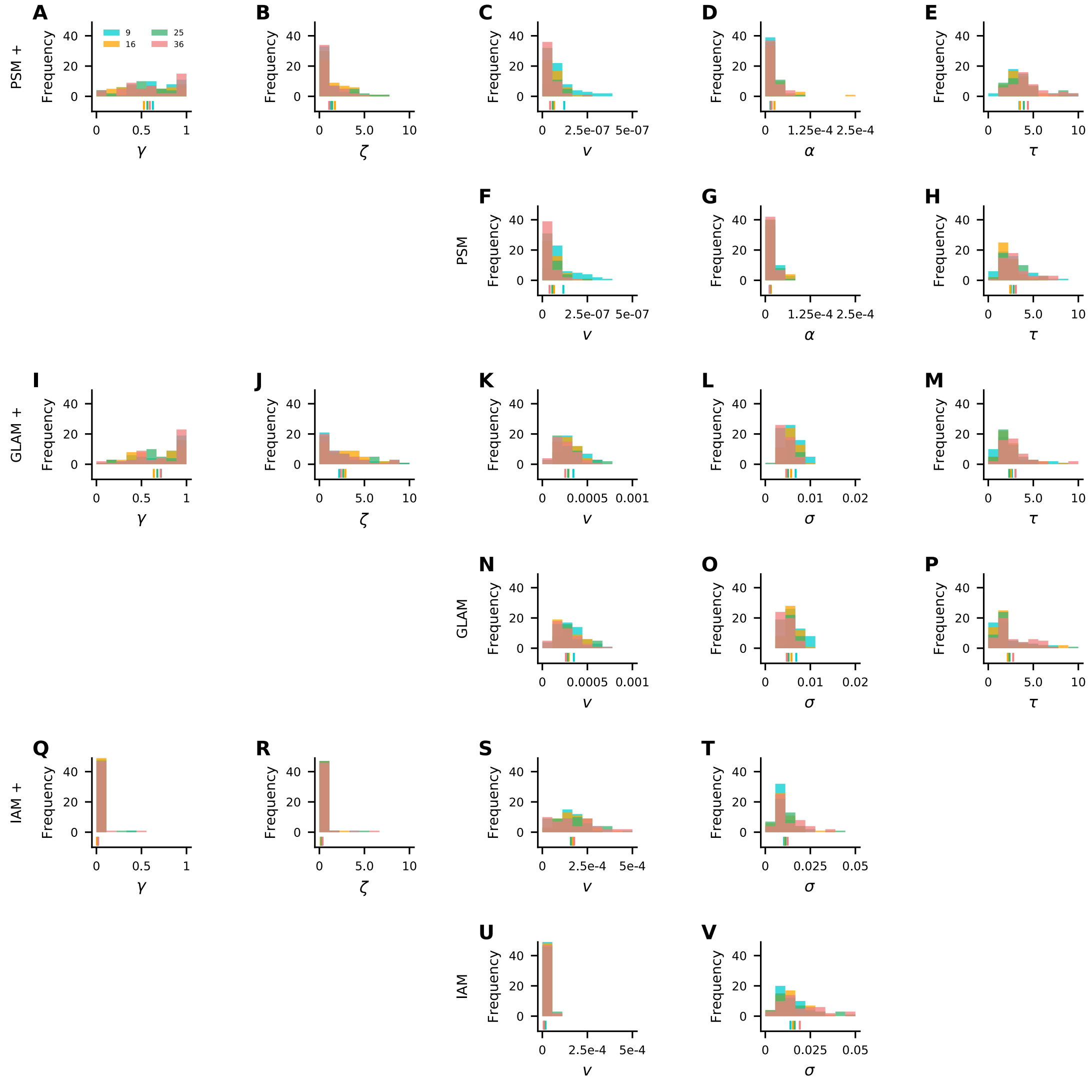

Figure 5-figure supplement 1. Parameter estimates from the in-sample fits of the probabilistic satisficing model (active gaze variant: A-E, passive gaze variant: F-H), GLAM (active gaze variant: I-M, passive gaze variant: N-P), and independent evidence accumulation model (active gaze variant: Q-T, passive gaze variant: U-V). Colors indicate choice set sizes. Vertical lines on the x-axis indicate the mean parameter estimate in each set size. For a detailed overview of the mean parameter estimates per model and choice set size, see Supplementary Materials 5-7.

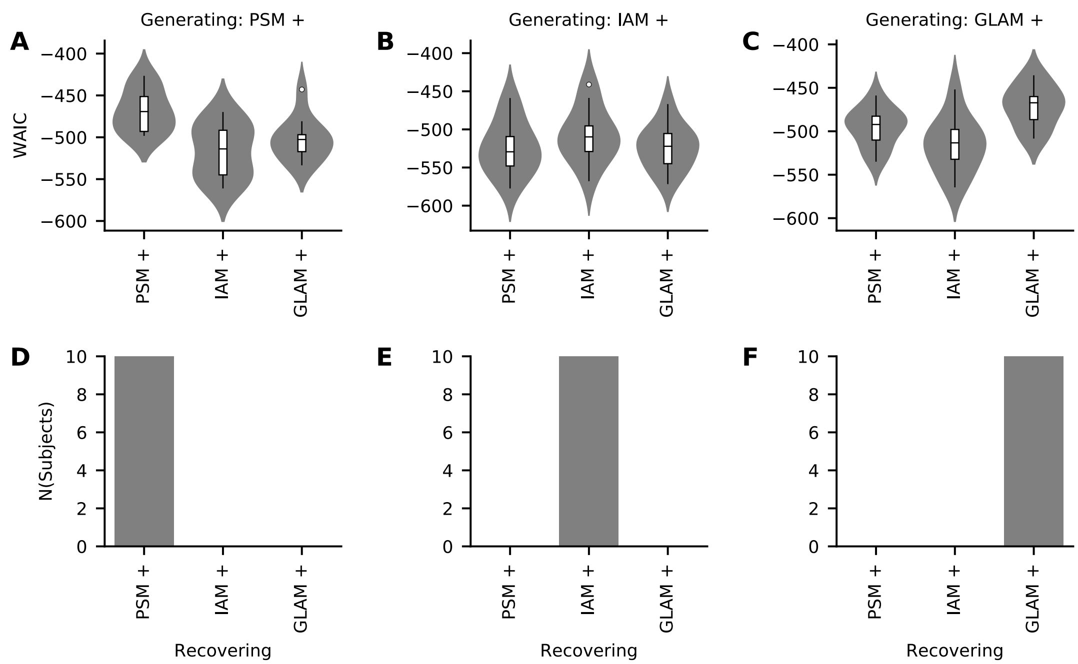

Figure 5-figure supplement 2. Model recovery. The goal of this analysis was to determine whether the three models with an active account of gaze (PSM+, IAM+, and GLAM+; see the "Methods" section of the main text) can be distinguished from one another in our dataset. Testing this is necessary to ensure that we can accurately identify the data-generating process. To test this, we selected 10 random subjects from our dataset and simulated choice and RT data for each of their 9-item trials (using the best-fitting individual parameters (see Figure 5-figure supplement 1)). Subsequently, we fitted the three models to each simulated dataset and compared their fit by means of the Widely Applicable Information Criterion (WAIC; Vehtari et al., 2017) (A-C). The WAIC is based on the log-score of the expected pointwise predictive density such that larger values in WAIC indicate better model fit. Each model consistently best captured its own predictions (D-F), indicating that the three models can be distinguished from one another. For details on the model simulation and fitting procedures, see the "Methods" section of the main text. Violin plots show a kernel density estimate of the distribution of individual values with boxplots inside of them.